

Generalization error bounds for DECONET: a deep unfolding network for analysis Compressive Sensing

Vasiliki Kouni

*Department of Informatics & Telecommunications
National & Kapodistrian University of Athens, Greece
Email: vicky-kouni@di.uoa.gr*

Abstract

In this paper, we propose a new deep unfolding network – based on a state-of-the-art optimization algorithm – for analysis Compressed Sensing. The proposed network called Decoding Network (DECONET) implements a decoder that reconstructs vectors from their incomplete, noisy measurements. Moreover, DECONET jointly learns a redundant analysis operator for sparsification, which is shared across the layers of DECONET. We study the generalization ability of DECONET. Towards that end, we first estimate the Rademacher complexity of the hypothesis class consisting of all the decoders that DECONET can implement. Then, we provide generalization error bounds, in terms of the aforementioned estimate. Finally, we present numerical experiments which confirm the validity of our theoretical results.

1 Introduction

Compressed Sensing (CS) [1] is a modern technique to reconstruct signals $x \in \mathbb{R}^n$ from few linear and possibly corrupted observations $y = Ax + e \in \mathbb{R}^m$, $m < n$. Iterative methods applied on CS are by now widely used [2, 3, 4]. Nevertheless, deep neural networks (DNNs) have become very popular for tackling sparse recovery problems like CS [5, 6], since they significantly reduce the time complexity and increase the quality of the reconstruction. A new line of research lies on merging DNNs and iterative optimization algorithms, leading to the so-called *deep unfolding/unrolling* [7, 8]. The latter pertains to interpreting the iterations of well-known iterative algorithms as layers of a DNN (called a *deep unfolding network*), which reconstructs the signals from their measurements.

1.1 Related work

Deep unfolding networks have become increasingly popular in the last few years [9], [10], [11], because of some advantages they have compared to traditional DNNs: they are interpretable, integrate prior knowledge about the signal structure [12], and have relatively few trainable parameters [13]. Especially in the case of CS, many unfolding networks have proven to work particularly well. For example, [14], [15, 16], [17], [18] interpret the iterations of approximate message passing (AMP) [19], iterative soft-thresholding (ISTA) [2], alternating direction method of multipliers (ADMM) [4] and fixed-point continuation (FPC) [20] algorithms, respectively, as layers of a neural network, which learns a *decoder* for CS, i.e., a function that reconstructs x from y . Additionally, such networks may jointly learn one, or more than one, from the following: a) step-sizes and/or thresholds used by the original iterative schemes b) the measurement matrix A c) a transform that sparsely represents x . The sparsifying transform may either be a square matrix [17], further constrained to be orthogonal [21] – integrating that way a dictionary learning technique – or a nonlinear transform, e.g. a combination of linear convolutional operators, separated by a rectified linear unit (ReLU) [15]. Dictionary learning has proven itself very useful when combined with model-based methods for CS [22, 23, 24]. Therefore, it seems natural to evolve unfolding networks that learn both the sparsifying dictionary and the decoder for CS.

Despite their empirical success, research community focuses lately on the study of the mathematical properties of unfolding networks. For example, [25, 26] provide convergence guarantees regarding variants of learned ISTA networks, while [11] studies the robustness of an unfolding network, produced by a forward-backward proximal interior point method. Moreover, [21, 27, 28] present generalization error bounds, in terms of the Rademacher complexity of the hypothesis class consisting of the functions that a learnable ISTA network can implement. The concept of generalization error bounds is widely known in the field of statistical learning theory and studied by different – albeit connected – complexity terms, such as Rademacher complexity [29], Vapnik-Chervonenkis (VC) dimension [30], stability [31] and robustness [32].

1.2 Motivation

Our work is inspired by [17], [21], [33]. Both [17] and [33] interpret the iterations of ADMM as layers of a neural network, which learns a decoder reconstructing the signals of interest from their (noisy) measurements. In [17], the decoder is jointly learned with a square sparsifying dictionary – initialized as a discrete cosine transform – and the thresholds employed in the original ADMM. Then, the proposed framework is tested on real-world MRI images. The ADMM-based decoder of [33] is jointly learned with a redundant sparsifying analysis operator – thus employing analysis sparsity in CS [34] – and is tested on real-world image and speech datasets. The unfolding network designed in [21] jointly learns an ISTA-based decoder and an orthogonal sparsifying dictionary – hence

imposing a synthesis sparsity model in CS [35]. Moreover, the authors provide a generalization error bound for the hypothesis class consisting of the functions that their ISTA-net learns. In the end, they evaluate their theoretical results, by testing their proposed decoder on synthetic signals and the MNIST dataset [36].

In a similar spirit, we derive a decoder for analysis-sparsity-based CS (from now on called *analysis CS*) by interpreting the iterations of the analysis- l_1 algorithm of [37] as layers of a DNN, which we call Decoding Network (*DECONET*). DECONET jointly learns a redundant sparsifying analysis operator, combining that way a dictionary learning technique. We prefer to employ analysis sparsity instead of synthesis sparsity in CS, due to some advantages the former has compared to the latter. For example, analysis sparsity provides flexibility in modelling sparse signals, by leveraging the redundancy of the involved analysis operators (we refer to Section 2 for a detailed comparison between the two models). Among other optimization methods handling analysis sparsity, our choice of [37] is attributed to its optimal performance. From the mathematical point of view, we study the generalization ability of DECONET. To that end, we estimate the generalization error achieved by DECONET, in terms of the empirical Rademacher complexity of the hypothesis class consisting of all the functions/decoders DECONET can implement. To the best of our knowledge, we are the first to study the generalization ability of an unfolding network, that jointly learns a CS decoder and a redundant sparsifier. In the end, we evaluate our theoretical results by testing our proposed framework on two real-world image datasets.

1.3 Key contributions

Our key contributions are listed below.

1. We build a new deep unfolding network dubbed DECONET, which jointly learns a) a decoder that solves the analysis CS problem b) a redundant analysis operator $W \in \mathbb{R}^{N \times n}$ ($N > n$) – shared across the layers of DECONET – for sparsification.
2. We introduce the hypothesis class – parameterized by W – of all the decoders DECONET can realize and restrict W to be bounded in this class. On one hand, the boundedness of the learnable W imposes a realistic structural constraint for the operator itself, that facilitates the estimation of the generalization error. On the other hand, the weight sharing assumption for W leads us to a recurrent neural network with a moderate number of weights.
3. We estimate the empirical Rademacher complexity of the aforementioned hypothesis class and use this estimate to derive meaningful generalization error bounds for DECONET. Our results showcase that the redundancy of W and the number of layers L affect the generalization ability of DECONET; roughly speaking, the generalization error scales like \sqrt{NL} .

4. We confirm the validity of our theoretical guarantees by testing DECONET on real-world image datasets. Furthermore, we compare DECONET to an ISTA-net baseline [21]; the latter jointly learns a decoder and an orthogonal sparsifier. Our experiments demonstrate that a) the generalization error of DECONET scales correctly with our theoretical findings b) DECONET outperforms the baseline in terms of the generalization error. This behaviour confirms improved performance when learning a redundant sparsifying transform instead of an orthogonal one.

1.4 Organization of the paper

The rest of the paper is outlined as follows. In Section 2, we briefly introduce CS, compare synthesis to analysis sparsity model and present example algorithms that solve CS under each sparsity model. In Section 3, we interpret a state-of-the-art iterative algorithm for analysis CS as a neural network coined DECONET, formulate its associated hypothesis class and define the empirical Rademacher complexity of the latter. Section 4 is dedicated to boundedness results, which are then used in Section 5 to deliver our main Theorems; the latter provide meaningful upper bounds on the generalization error of DECONET. Section 6 is devoted to numerical experiments, where we evaluate our framework under multiple settings. Finally, we conclude in Section 7, wrapping up and giving some potential future directions.

1.5 Notation

We denote the cardinality of a set S by $|S|$. For $n \in \mathbb{N}$, we write $[n]$ for the set of indices $\{1, 2, \dots, n\}$. We denote the set of real, positive numbers by \mathbb{R}_+ . For a sequence a_n that is upper bounded by $M > 0$, we write $\{a_n\} \leq M$; similarly if it is lower bounded. The support of a vector $x \in \mathbb{R}^n$ is the index set of its nonzero entries and is denoted by $\text{supp}(x)$, i.e. $\text{supp}(x) = \{i \in [n] : x_i \neq 0\}$. For a matrix $A \in \mathbb{R}^{n \times n}$, we write $\|A\|_{2 \rightarrow 2}$ for its operator/spectral norm and $\|A\|_F$ for its Frobenius norm. For a family of vectors $(\phi_i)_{i=1}^N$ in \mathbb{R}^n , its associated analysis operator is given by $\Phi f := \{\langle f, \phi_i \rangle\}_{i=1}^N$, where $f \in \mathbb{R}^n$. Its synthesis operator is simply the adjoint Φ^T . For matrices $A_1, A_2 \in \mathbb{R}^{N \times N}$, we denote by $[A_1; A_2] \in \mathbb{R}^{2N \times N}$ their concatenation with respect to the first dimension, while we denote by $[A_1 | A_2] \in \mathbb{R}^{N \times 2N}$ their concatenation with respect to the second dimension. We write $O_{N \times N}$ for a real-valued $N \times N$ matrix filled with zeros. We denote by $\text{diag}(\alpha)$ the square diagonal matrix having $\alpha \in \mathbb{R}$ in its main diagonal and zero elsewhere. For $x \in \mathbb{R}$, $\tau > 0$, the soft thresholding operator $\mathcal{S}_\tau : \mathbb{R} \mapsto \mathbb{R}$ is defined as

$$\mathcal{S}_\tau(x) = \mathcal{S}(x, \tau) = \begin{cases} \text{sign}(x)(|x| - \tau), & |x| \geq \tau \\ 0, & \text{otherwise} \end{cases}, \quad (1)$$

or in closed form $\mathcal{S}(x, \tau) = \text{sign}(x) \max(0, |x| - \tau)$. For $x \in \mathbb{R}^n$, the soft thresholding operator acts componentwise, i.e. $(\mathcal{S}_\tau(x))_i = \mathcal{S}_\tau(x_i)$. For $y \in \mathbb{R}^n$, $\tau > 0$,

the mapping

$$P_G(\tau; y) = \operatorname{argmin}_{x \in \mathbb{R}^n} \left\{ \tau G(x) + \frac{1}{2} \|x - y\|_2^2 \right\}, \quad (2)$$

is called the *proximal mapping associated to the convex function* G . In fact, for $G = \|\cdot\|_1$, (2) coincides with (1). For $x \in \mathbb{R}$, $\tau > 0$, the truncation operator $\mathcal{T}_\tau : \mathbb{R} \mapsto \mathbb{R}$ is defined as

$$\mathcal{T}_\tau(x) = \mathcal{T}(x, \tau) = \operatorname{sign}(x) \min\{|x|, \tau\} = \begin{cases} \tau \operatorname{sign}(x), & |x| \geq \tau \\ x, & \text{otherwise} \end{cases} \quad (3)$$

For $x \in \mathbb{R}^n$, the truncation operator acts componentwise and is 1-Lipschitz. The epigraph of the l_2 -norm is the set $\mathcal{L}_2^n = \{(x, t) \in \mathbb{R}^{n+1} : \|x\|_2 \leq t\}$. For two functions $f, g : \mathbb{R}^n \mapsto \mathbb{R}^n$, we write their composition as $f \circ g : \mathbb{R}^n \mapsto \mathbb{R}^n$ and if there exists some constant $C > 0$ such that $f(x) \leq Cg(x)$, then we write $f(x) \lesssim g(x)$. The covering number $\mathcal{N}(T, \|\cdot\|, t)$ of a space T , equipped with a norm $\|\cdot\|$, at level $t > 0$, is defined as the smallest number of balls of radius t with respect to $\|\cdot\|$, required to cover T . For the ball of radius $t > 0$ in \mathbb{R}^n , we write $B_{\|\cdot\|_2}^n(t)$. For $\Lambda > 0$, the set of all matrices $W \in \mathbb{R}^{N \times n}$ with bounded – by Λ – spectral norm is defined as $\mathcal{B}_\Lambda = \{W \in \mathbb{R}^{N \times n} \mid \exists \Lambda > 0 \text{ such that } \|W\|_{2 \rightarrow 2} \leq \Lambda\}$.

2 Optimization-based Compressed Sensing

2.1 Synthesis Sparsity in CS

As mentioned in Section 1, the main idea of CS is to reconstruct a vector $x \in \mathbb{R}^n$ from $y = Ax + e \in \mathbb{R}^m$, $m < n$, where A is the so-called *measurement matrix* [38] and $e \in \mathbb{R}^m$, with $\|e\| \leq \varepsilon$, corresponds to noise, with $\varepsilon > 0$ being an estimate on the noise level. In order to ensure exact/approximate reconstruction of x , we rely on two facts. First, A must meet some conditions, for example the restricted isometry property or the null space property [38]. Second, we impose a *sparse data model* to x [39]. Sparse data models are split in synthesis and analysis sparsity [35]. In the former [40, 38, 41, 42], signals are considered to be sparse when *synthesized* by a few column vectors taken from a large matrix (*dictionary*) $D \in \mathbb{R}^{p \times n}$ ($p \leq n$). Moreover, D is usually an orthogonal transform, e.g. a wavelet or DCT matrix $D \in \mathbb{R}^{n \times n}$. Now, employing synthesis sparsity in CS, with $D \in \mathbb{R}^{n \times n}$, we aim to recover x from y . A common way to do so is by solving the l_1 -*minimization* problem

$$\min_{z \in \mathbb{R}^n} \|z\|_1 \quad \text{subject to} \quad \|y - ADz\|_2 \leq \varepsilon. \quad (4)$$

Towards that end, numerous iterative algorithms [2, 3, 43] have emerged. Typically, they consist of an iterative scheme that incorporates a proximal mapping and after a number of iterations and under certain conditions, they converge to

a minimizer \hat{x} of (4). For example, ISTA uses the proximal mapping¹ (2) to yield the following iterative scheme

$$\begin{aligned} z_{k+1} &= \mathcal{S}_{\tau\lambda}(z_k + \tau(AD)^T(y - ADz)) \\ z_{k+1} &= \mathcal{S}_{\tau\lambda}((I - D^T A^T AD)z + \tau(AD)^T z), \end{aligned} \quad (5)$$

for $k = 0, 1, \dots$, $z_0 = 0$, with $\tau, \lambda > 0$ being parameters of the algorithm. If $\tau\|AD\|_{2 \rightarrow 2}^2 \leq 1$ [44], z_k converges to a minimizer \hat{z} of (4), so that the reconstructed \hat{x} is simply given by $\hat{x} = D\hat{z}$.

2.2 Analysis Sparsity in CS

Despite its success, synthesis sparsity has a “twin”, i.e., the *analysis sparsity model* [45, 34, 46] (also known as *co-sparse model* [46, 47]), in which we assume that there exists a *redundant analysis operator* $W \in \mathbb{R}^{N \times n}$ ($N > n$), so that Wx is sparse. The associated optimization problem for CS is the *analysis l_1 -minimization* problem

$$\min_{x \in \mathbb{R}^n} \|Wx\|_1 \quad \text{subject to} \quad \|Ax - y\|_2 \leq \varepsilon \quad (6)$$

and from now on, whenever we speak about the redundancy of such an analysis operator, we mean the number of its rows N .

Analysis sparsity has become popular, due to some benefits it has compared to its synthesis counterpart. For example, it is computationally more appealing to solve the optimization algorithm of analysis CS, since the actual optimization takes place in the ambient space [48] and the algorithm involved may need less measurements for perfect reconstruction, if one uses a redundant transform instead of an orthogonal one [45].

Nevertheless, choosing the appropriate iterative algorithm for solving (6) may be a tricky task. The reason is that most thresholding algorithms cannot handle analysis sparsity, since the proximal mapping associated to $\|W(\cdot)\|_1$ does not have a closed-form type. Hence, if we want to perform analysis CS, we have to come up with another iterative method. To tackle this issue, we choose the state-of-the-art l_1 -analysis algorithm described in [37], which employs a conic formulation methodology. For reasons of convenience, we will refer to the aforementioned algorithm as *analysis conic form* (ACF) from now on. We will briefly describe the steps leading to the derivation of ACF, as these are stated in [37]. First, the authors of [37] determine an equivalent to (6) smoothed conic formulation, i.e.

$$\min_{x \in \mathbb{R}^n} \|Wx\|_1 + \frac{\mu}{2} \|x - x_0\|_2^2 \quad \text{subject to} \quad (y - Ax, \varepsilon) \in \mathcal{L}_2^m, \quad (7)$$

where $\mu \in \mathbb{R}_+$ is an adequate smoothing parameter, $x_0 \in \mathbb{R}^n$ is an initial guess on x and \mathcal{L}_2^m is the epigraph of the l_2 -norm. Second, they determine the dual

¹we remind that the proximal mapping with respect to $\|\cdot\|_1$ coincides to the soft thresholding operator (1)

of (7) to be

$$\begin{aligned}
& \text{maximize} && \langle y, z^2 \rangle - \varepsilon \|z^2\|_2 \\
& \text{subject to} && A^T z^2 - W^T z^1 = 0 \\
& && \|z^1\|_\infty \leq 1,
\end{aligned} \tag{8}$$

where $z^1 \in \mathbb{R}^N$, $z^2 \in \mathbb{R}^m$ are dual variables. After presenting a collection of arguments and computations, they end up with Algorithm 1 – being a variant of an optimal first-order method – stated below, with a step size multiplier $0 < \{\theta_k\} \leq 1$.

Algorithm 1: ACF

Input : $x_0 \in \mathbb{R}^n$, $z_0^1 \in \mathbb{R}^N$, $z_0^2 \in \mathbb{R}^m$, $\mu \in \mathbb{R}_+$, step sizes $\{t_k^1\}$, $\{t_k^2\}$
Output: solution \hat{x}_μ of (7)

- 1 $\theta_0 \leftarrow 1$, $u_0^1 = z_0^1$, $u_0^2 = z_0^2$;
- 2 **for** iterations $k = 0, 1, \dots$ **do**
- 3 $x_k \leftarrow x_0 + \mu^{-1}((1 - \theta_k)W^T u_k^1 + \theta_k W^T z_k^1 - (1 - \theta_k)A^T u_k^2 - \theta_k A^T z_k^2)$;
- 4 $z_{k+1}^1 \leftarrow \mathcal{T}((1 - \theta_k)u_k^1 + \theta_k z_k^1 - \theta_k^{-1} t_k^1 W x_k, \theta_k^{-1} t_k^1)$;
- 5 $z_{k+1}^2 \leftarrow \mathcal{S}((1 - \theta_k)u_k^2 + \theta_k z_k^2 - \theta_k^{-1} t_k^2 (y - A x_k), \theta_k^{-1} t_k^2 \varepsilon)$;
- 6 $u_{k+1}^1 \leftarrow (1 - \theta_k)u_k^1 + \theta_k z_{k+1}^1$;
- 7 $u_{k+1}^2 \leftarrow (1 - \theta_k)u_k^2 + \theta_k z_{k+1}^2$;
- 8 $\theta_{k+1} \leftarrow 2/(1 + (1 + 4/(\theta_k)^2)^{1/2})$;
- 9 **end**

The dual function g_μ corresponding to (8) has a Lipschitz continuous gradient, hence ACF converges [37] to a solution \hat{x}_μ of (7), for which we have $\hat{x}_\mu \xrightarrow{\mu \rightarrow 0} \hat{x}$, where \hat{x} is an optimal solution of (6). The authors of [37] clarify that when they speak about the optimal solution \hat{x} , they refer to this uniquely determined value. Additionally, they argue that there are situations where \hat{x} and \hat{x}_μ coincide. Henceforward, we stick to their formulation and simply speak about the solution \hat{x} .

We will see in the next Section how ACF may be interpreted as a neural network with L layers/iterations.

3 A deep unfolding network for Compressed Sensing

3.1 Neural network formulation of the iterative algorithm

We consider a standard scenario for the ACF, where $z_0^1 = u_0^1 = 0$, $z_0^2 = u_0^2 = 0$, $t_0^1 = t_0^2 = \theta_0 = 1$, $0 < \{t_k^1\}, \{t_k^2\}, \{\theta_k\} \leq 1$, $x_0 = A^T y$. We substitute first x -update into z^1 - and z^2 -updates and second z^1 - and z^2 - into u^1 - and

u^2 -updates, respectively, concatenate $z_k^1, z_k^2, u_k^1, u_k^2$ in one vector v_k , i.e.

$$v_k = \begin{pmatrix} z_k^1 \\ z_k^2 \\ u_k^1 \\ u_k^2 \end{pmatrix} \in \mathbb{R}^{(2N+2m) \times 1} \quad \text{for } k \geq 0, \quad (9)$$

with $v_0 = 0$, and do the calculations, so that

$$v_k = D_{k-1}v_{k-1} + \Theta_{k-1} \begin{pmatrix} \mathcal{T}(G_{k-1}^1 v_{k-1} - b_{k-1}^1, \theta_{k-1}^{-1} t_{k-1}^1) \\ \mathcal{S}(G_{k-1}^2 v_{k-1} - b_{k-1}^2, \theta_{k-1}^{-1} t_{k-1}^2 \varepsilon) \\ \mathcal{T}(G_{k-1}^1 v_{k-1} - b_{k-1}^1, \theta_{k-1}^{-1} t_{k-1}^1) \\ \mathcal{S}(G_{k-1}^2 v_{k-1} - b_{k-1}^2, \theta_{k-1}^{-1} t_{k-1}^2 \varepsilon) \end{pmatrix}, \quad (10)$$

where

$$D_k = \text{diag}(\underbrace{1 - \theta_0, \dots, 1 - \theta_0}_{N+m \text{ times}}, \underbrace{1 - \theta_k, \dots, 1 - \theta_k}_{N+m \text{ times}}) \in \mathbb{R}^{(2N+2m) \times (2N+2m)}, \quad (11)$$

$$\Theta_k = \text{diag}(\underbrace{\theta_0, \dots, \theta_0}_{N+m \text{ times}}, \underbrace{\theta_k, \dots, \theta_k}_{N+m \text{ times}}) \in \mathbb{R}^{(2N+2m) \times (2N+2m)}, \quad (12)$$

$$G_k^1 = (\theta_k (I - \theta_k^{-1} t_k^1 \mu^{-1} W W^T) \mid t_k^1 \mu^{-1} W A^T \mid (1 - \theta_k) \cdot (I - \theta_k^{-1} t_k^1 \mu^{-1} W W^T) \mid (1 - \theta_k) \theta_k^{-1} t_k^1 \mu^{-1} W A^T) \in \mathbb{R}^{N \times (2N+2m)}, \quad (13)$$

$$G_k^2 = (t_k^2 \mu^{-1} A W^T \mid \theta_k (I - \theta_k^{-1} t_k^2 \mu^{-1} A A^T) \mid (1 - \theta_k) \theta_k^{-1} t_k^2 \mu^{-1} A W^T \mid (1 - \theta_k) (I - \theta_k^{-1} t_k^2 \mu^{-1} A A^T)) \in \mathbb{R}^{m \times (2N+2m)}, \quad (14)$$

$$b_k^1 = \theta_k^{-1} t_k^1 W x_0 \in \mathbb{R}^N, \quad (15)$$

$$b_k^2 = \theta_k^{-1} t_k^2 (y - A x_0) \in \mathbb{R}^m. \quad (16)$$

We observe that (10) can be interpreted as a layer of a neural network, with weights G^1, G^2 , biases b^1, b^2 and activation functions \mathcal{T}, \mathcal{S} . Nevertheless, this interpretation of ACF as a DNN does not account for any trainable parameters. We cope with this issue by considering W to be a) unknown b) bounded with respect to the operator norm, i.e. $W \in \mathcal{B}_\Lambda$, for some $\Lambda > 0$ c) learned from a training sequence $\mathcal{S} = \{(x_i, y_i)\}_{i=1}^s$ with i.i.d. samples drawn from an unknown distribution² \mathcal{D}^s . Hence, the trainable parameters are the entries of W and W is shared across the layers.

Now, based on (10), we formulate ACF as a neural network with L layers/iterations, defined as

$$f_1(y) = \sigma(y) \quad (17)$$

$$f_k(v) = D_{k-1}v + \Theta_{k-1}\sigma(v), \quad k = 2, \dots, L, \quad (18)$$

where

$$\sigma(y)^T = (\mathcal{T}(-t_0^1 W x_0, t_0^1), \mathcal{S}(t_0^2 (y - A x_0), t_0^2 \varepsilon), \mathcal{T}(-t_0^1 W x_0, t_0^1), \mathcal{S}(t_0^2 (y - A x_0), t_0^2 \varepsilon))^T, \quad (19)$$

²formally speaking, this is a distribution over the x_i and then $y_i = A x_i + e$, with fixed A, e

$$\begin{aligned} \sigma(v)^T &= (\mathcal{T}(G_k^1 v - b_k^1), \mathcal{S}(G_k^2 v - b_k^2), \\ &\quad \mathcal{T}(G_k^1 v - b_k^1), \mathcal{S}(G_k^2 v - b_k^2))^T, \quad k = 2, \dots, L. \end{aligned} \quad (20)$$

We denote the composition of L such layers (all having the same W) as

$$f_W^L(y) = f_L \circ f_{L-1} \circ \dots \circ f_1(y). \quad (21)$$

The latter constitutes the realization of a neural network with L layers, that reconstructs v from y . Thus, we call (21) an *intermediate decoder*, since it is not the final form of the decoder we wish to derive. Towards this end, in order to get the solution \hat{x} , we apply an affine map $\phi : \mathbb{R}^{(2N+2m) \times 1} \mapsto \mathbb{R}^{n \times 1}$ – motivated by the x -update of ACF – after the last layer L , so that

$$\hat{x} := \phi(v) = \Phi v + x_0, \quad (22)$$

where

$$\begin{aligned} \Phi &= (\mu^{-1}\theta_L W^T | -\mu^{-1}\theta_L A^T \\ &\quad | \mu^{-1}(1 - \theta_L)W^T | -\mu^{-1}(1 - \theta_L)A^T) \in \mathbb{R}^{n \times (2N+2m)}. \end{aligned} \quad (23)$$

Moreover, in order to clip the output $\phi(f_W^L(y))$ in case its norm falls out of a reasonable range, we add an extra function $\psi : \mathbb{R}^n \rightarrow \mathbb{R}^n$ after the application of the affine map ϕ and define it as

$$\psi(x) = \begin{cases} x, & \|x\|_2 \leq B_{\text{out}} \\ B_{\text{out}} \frac{x}{\|x\|_2}, & \text{otherwise} \end{cases}, \quad (24)$$

for some fixed constant $B_{\text{out}} > 0$. Now, for a fixed number of layers L , the desired learnable decoder is written as

$$\text{dec}_W^L(y) = \psi(\phi(f_W^L(y))). \quad (25)$$

We call DECONET (DECODing NETwork) the neural network that implements such a decoder. Notice that the latter is parameterized by W , since W is shared across the layers of DECONET.

3.2 Defining the hypothesis class and the Rademacher complexity

We introduce the hypothesis class

$$\mathcal{H}^L = \{h : \mathbb{R}^m \mapsto \mathbb{R}^n : h(y) = \psi(\phi(f_W^L(y))), W \in \mathcal{B}_\Lambda\}, \quad (26)$$

parameterized by W and consisting of all the functions/decoders DECONET can implement. Given (26) and the training set \mathcal{S} , DECONET yields a function $h_{\mathcal{S}} \in \mathcal{H}^L$ that aims at reconstructing x from y . For a loss function $\ell : \mathcal{H}^L \times$

$\mathbb{R}^n \times \mathbb{R}^m \mapsto \mathbb{R}_+$, the empirical loss of a hypothesis $h_{\mathcal{S}}$ is the reconstruction error on the training set, i.e.

$$\hat{\mathcal{L}}_{train}(h_{\mathcal{S}}) = \frac{1}{s} \sum_{i=1}^s \ell(h_{\mathcal{S}}, x_i, y_i). \quad (27)$$

In this paper, we choose as loss function ℓ the squared l_2 -norm, since a) it is considered a typical measure of reconstruction error in regression-style problems like CS b) we prefer to be consistent with the forthcoming numerical experiments, where we train DECONET with respect to $\|\cdot\|_2^2$. Now, the empirical loss takes the form of the training *mean-squared error* (MSE)

$$\hat{\mathcal{L}}_{train}(h_{\mathcal{S}}) = \frac{1}{s} \sum_{j=1}^s \|h_{\mathcal{S}}(y_j) - x_j\|_2^2. \quad (28)$$

The true loss is

$$\mathcal{L}(h_{\mathcal{S}}) = \mathbb{E}_{(x,y) \sim \mathcal{D}} (\|h_{\mathcal{S}}(y) - x\|_2^2). \quad (29)$$

The generalization error is given as the difference³ between the empirical and true loss

$$GE(h_{\mathcal{S}}) = |\hat{\mathcal{L}}_{train}(h_{\mathcal{S}}) - \mathcal{L}(h_{\mathcal{S}})|. \quad (30)$$

A typical way to estimate (30) consists in upper bounding it in terms of the *Rademacher complexity*. The *empirical Rademacher complexity* is defined as

$$\mathcal{R}_{\mathcal{S}}(\ell \circ \mathcal{H}^L) = \mathbb{E} \sup_{h \in \mathcal{H}^L} \frac{1}{s} \sum_{i=1}^s \epsilon_i \|h(y_i) - x_i\|_2^2, \quad (31)$$

where ϵ is a Rademacher vector, that is, a vector with entries taking the values ± 1 with equal probability. Then, the Rademacher complexity is defined as

$$\mathcal{R}_s(\ell \circ \mathcal{H}^L) = \mathbb{E}_{\mathcal{S} \sim \mathcal{D}^s} (\mathcal{R}_{\mathcal{S}}(\ell \circ \mathcal{H}^L)). \quad (32)$$

In this paper, we solely work with (31). We rely on the following Theorem that estimates (30) in terms of (31).

Theorem 3.1. *Let \mathcal{H} be a family of functions, \mathcal{S} the training set drawn from \mathcal{D}^s , and ℓ a real-valued bounded loss function satisfying $|\ell(h, z)| \leq c$, for all $h \in \mathcal{H}$, $z \in Z$. Then, for $\delta \in (0, 1)$, with probability at least $1 - \delta$, we have for all $h \in \mathcal{H}$*

$$\mathcal{L}(h) \leq \hat{\mathcal{L}}(h) + 2\mathcal{R}_{\mathcal{S}}(\ell \circ \mathcal{H}) + 4c \sqrt{\frac{2 \log(4\delta)}{s}}. \quad (33)$$

In order to use the previous Theorem, the loss function must be bounded. Towards this end, we make two reasonable (for the machine learning literature)

³some of the existing literature denotes the true loss as the generalization error, but the definition we give in (30) is more convenient for our purposes

assumptions regarding the training set $\mathcal{S} = \{(x_i, y_i)\}_{i=1}^s$. Let us suppose that with overwhelming probability we have

$$\|y_i\|_2 \leq B_{\text{in}}, \quad (34)$$

for some constant $B_{\text{in}} > 0$, $i = 1, \dots, s$. Moreover, we assume that for any $h \in \mathcal{H}^L$, with overwhelming probability over y_i chosen from \mathcal{D} , the following holds

$$\|h(y_i)\|_2 \leq B_{\text{out}}, \quad (35)$$

by definition of ψ , for some constant $B_{\text{out}} > 0$, for all $i = 1, \dots, s$. Hence, the loss function is bounded as $\|h(y_i) - x_i\|_2^2 \leq (B_{\text{in}} + B_{\text{out}})^2$, for all $i = 1, \dots, s$. Following the previous assumptions, it is easy to check that $\|\cdot\|_2^2$ is a Lipschitz function, with Lipschitz constant $\text{Lip}_{\|\cdot\|_2^2} = 2B_{\text{in}} + 2B_{\text{out}}$.

The Lipschitzness of $\|\cdot\|_2^2$ allows us to remove the loss function in (31) and study $\mathcal{R}_{\mathcal{S}}(\mathcal{H})$ alone. To do so, we employ the so-called (vector-valued) contraction principle [49].

Lemma 3.2. *Let \mathcal{H} be a set of function $h : \mathcal{X} \mapsto \mathbb{R}^n$, $f : \mathbb{R}^n \mapsto \mathbb{R}^n$ a K -Lipschitz function and $\mathcal{S} = \{x_i\}_{i=1}^s$. Then*

$$\mathbb{E} \sup_{h \in \mathcal{H}} \sum_{i=1}^s \epsilon_i f \circ h(x_i) \leq \sqrt{2}K \mathbb{E} \sup_{h \in \mathcal{H}} \sum_{i=1}^s \sum_{k=1}^n \epsilon_{ik} h_k(x_i), \quad (36)$$

where $(\epsilon_i), (\epsilon_{ik})$ are both Rademacher sequences.

We apply the previous Lemma to (31), yielding

$$\begin{aligned} \mathcal{R}_s(l \circ \mathcal{H}^L) &\leq \sqrt{2} \text{Lip}_{\|\cdot\|_2^2} \mathcal{R}_s(\mathcal{H}^L) = \sqrt{2} \text{Lip}_{\|\cdot\|_2^2} \mathbb{E} \sup_{h \in \mathcal{H}^L} \sum_{i=1}^s \sum_{k=1}^n \epsilon_{ik} h_k(x_i) \\ &= \sqrt{2} (2B_{\text{in}} + 2B_{\text{out}}) \mathbb{E} \sup_{h \in \mathcal{H}^L} \sum_{i=1}^s \sum_{k=1}^n \epsilon_{ik} h_k(x_i). \end{aligned} \quad (37)$$

We will come back to the estimation of (37) in Section 5, after presenting the adequate mathematical tools in Section 4. Towards that end, we loosely follow the mathematical strategy described in [21].

4 Boundedness results

We present a series of boundedness results that are essential for the estimation of the generalization error bounds.

4.1 Bounding outputs

We take into account the number of training samples and pass to matrix notation. Due to (34), (35) and the Cauchy-Schwartz inequality, we get

$$\|Y\|_F \leq \sqrt{s} B_{\text{in}} \quad (38)$$

$$\|h(Y)\|_F = \|\psi(\phi(f_W^L(Y)))\|_F \leq \sqrt{s} B_{\text{out}}. \quad (39)$$

We will make wide use of the following inequality, so we state it below as a Lemma.

Lemma 4.1. *Let $k \geq 0$. For any $W \in \mathcal{B}_\Lambda$, step sizes $\{t_k^1\}, \{t_k^2\} > 0$ with $t_0^1 = t_0^2 = 1$, step size multiplier $0 < \{\theta_k\} \leq 1$ with $\theta_0 = 1$, and smoothing parameter $\mu > 0$, the following holds for the matrices G_k^1, G_k^2 defined in (13), (14), respectively:*

$$2\|G_k^1\|_{2 \rightarrow 2} + 2\|G_k^2\|_{2 \rightarrow 2} + 1 \leq \Gamma_k, \quad (40)$$

where

$$\Gamma_k = 2[c_{1,k}\Lambda^2 + c_{2,k}\|A\|_{2 \rightarrow 2}^2 + 2\|A\|_{2 \rightarrow 2}\Lambda(c_{1,k} + c_{2,k})] + 1, \quad (41)$$

with $\Gamma_k \leq 6(\max\{\Lambda, \|A\|_{2 \rightarrow 2}\}^2(c_{1,k} + c_{2,k})) + 1$ and $c_{1,k} = \theta_k^{-1}\mu^{-1}t_k^1$, $c_{2,k} = \theta_k^{-1}\mu^{-1}t_k^2$, for all $k \geq 0$. Moreover, if $\{\theta_k\}, \{c_{1,k}\} \leq 1$, then

$$\Gamma_k \leq \gamma, \quad (42)$$

with $\gamma = 2(\Lambda^2 + \|A\|_{2 \rightarrow 2}^2 + 4\|A\|_{2 \rightarrow 2}\Lambda) + 1 > 1$.

Proof. Based on (13), (14), we get

$$\begin{aligned} & \|G_k^1\|_{2 \rightarrow 2} + \|G_k^2\|_{2 \rightarrow 2} \leq [\theta_k\|I - \theta_k^{-1}\mu^{-1}t_k^1WW^T\|_{2 \rightarrow 2} \\ & \quad + \mu^{-1}t_k^1\|W\|_{2 \rightarrow 2}\|A\|_{2 \rightarrow 2} + (1 - \theta_k)\|I - \theta_k^{-1}\mu^{-1}t_k^1WW^T\|_{2 \rightarrow 2} \\ & \quad \quad + (1 - \theta_k)\theta_k^{-1}\mu^{-1}t_k^1\|W\|_{2 \rightarrow 2}\|A\|_{2 \rightarrow 2}] \\ & \quad + [\mu^{-1}t_k^2\|A\|_{2 \rightarrow 2}\|W\|_{2 \rightarrow 2} + \theta_k\|I - \theta_k^{-1}\mu^{-1}t_k^2AA^T\|_{2 \rightarrow 2} + (1 - \theta_k) \\ & \quad \quad \cdot \theta_k^{-1}\mu^{-1}t_k^2\|A\|_{2 \rightarrow 2}\|W\|_{2 \rightarrow 2} + (1 - \theta_k)\|I - \theta_k^{-1}\mu^{-1}t_k^2AA^T\|_{2 \rightarrow 2}] \\ & = [\|I - \theta_k^{-1}\mu^{-1}t_k^1WW^T\|_{2 \rightarrow 2} + \|W\|_{2 \rightarrow 2}\|A\|_{2 \rightarrow 2}(\theta_k^{-1}\mu^{-1}t_k^1 + \mu^{-1}t_k^1)] \\ & \quad + [\|I - \theta_k^{-1}\mu^{-1}t_k^2AA^T\|_{2 \rightarrow 2} + \|W\|_{2 \rightarrow 2}\|A\|_{2 \rightarrow 2}(\theta_k^{-1}\mu^{-1}t_k^2 + \mu^{-1}t_k^2)]. \end{aligned}$$

Now, we define $c_{1,k} = \theta_k^{-1}\mu^{-1}t_k^1$, $c_{2,k} = \theta_k^{-1}\mu^{-1}t_k^2$, use the boundedness assumption of W and the fact that $\|I - c_{1,k}WW^T\|_{2 \rightarrow 2} \leq \max\{c_{1,k}\Lambda - 1, 1\} \leq c_{1,k}\Lambda$ to get

$$\begin{aligned} & 2\|G_k^1\|_{2 \rightarrow 2} + 2\|G_k^2\|_{2 \rightarrow 2} + 1 \\ & \leq 2[c_{1,k}\Lambda^2 + c_{2,k}\|A\|_{2 \rightarrow 2}^2 + \|A\|_{2 \rightarrow 2}\Lambda(c_{1,k} + \theta_k c_{1,k} + c_{2,k} + \theta_k c_{2,k})] + 1 \\ & \quad \stackrel{\theta_k \leq 1}{\leq} 2[c_{1,k}\Lambda^2 + c_{2,k}\|A\|_{2 \rightarrow 2}^2 + 2\|A\|_{2 \rightarrow 2}\Lambda(c_{1,k} + c_{2,k})] + 1. \quad (43) \end{aligned}$$

Now, we set $\Gamma_k = 2[c_{1,k}\Lambda^2 + c_{2,k}\|A\|_{2 \rightarrow 2}^2 + 2\|A\|_{2 \rightarrow 2}\Lambda(c_{1,k} + c_{2,k})] + 1$. If we take the maximum between $\|A\|_{2 \rightarrow 2}^2$ and Λ^2 , then

$$\begin{aligned} \Gamma_k & \leq 2[3c_{1,k}(\max\{\Lambda, \|A\|_{2 \rightarrow 2}\})^2 + 3c_{2,k}(\max\{\Lambda, \|A\|_{2 \rightarrow 2}\})^2] + 1 \\ & = 6(\max\{\Lambda, \|A\|_{2 \rightarrow 2}\})^2(c_{1,k} + c_{2,k}) + 1. \quad (44) \end{aligned}$$

Combining the latter with the fact that $\Gamma_k \geq 1$, for any $k \geq 0$, gives us the restriction of Γ_k in the desired interval. Moreover, if $\{c_{1,k}\}, \{c_{2,k}\} \leq 1$ for any $k \geq 0$, then we have the following simplified upper bound for Γ_k , that does not depend on k :

$$\Gamma_k \leq 2(\Lambda^2 + \|A\|_{2 \rightarrow 2}^2 + 4\|A\|_{2 \rightarrow 2}\Lambda) + 1.$$

We set $\gamma := 2(\Lambda^2 + \|A\|_{2 \rightarrow 2}^2 + 4\|A\|_{2 \rightarrow 2}\Lambda) + 1$ (obviously $\gamma > 1$) and the proof follows. \square

Apart from the boundedness results we have presented so far, we can upper-bound the output $f_W^k(Y)$ with respect to the Frobenius norm, after any number of layers k and especially for $k < L$, so that ϕ and ψ are not applied after the final layer L . The following Lemma will be needed later on, when we prove that $f_W^L(Y)$ is Lipschitz continuous with respect to W .

Lemma 4.2. *Let $k \in \mathbb{N}$. For any $W \in \mathcal{B}_\Lambda$, step sizes $\{t_k^1\}, \{t_k^2\} > 0$ with $t_0^1 = t_0^2 = 1$, $t_{-1}^1 = t_{-1}^2 = 0$, step size multiplier $0 < \{\theta_k\} \leq 1$ with $\theta_0 = \theta_{-1} = 1$, and smoothing parameter $\mu > 0$, the following holds for the output of the function f_W^k defined in (18):*

$$\begin{aligned} \|f_W^k(Y)\|_F \leq & 2\mu\|Y\|_F \sum_{i=0}^{k-1} \left(\left(\|A\|_{2 \rightarrow 2}(c_{1,i-1}\Lambda + c_{2,i-1}\|A\|_{2 \rightarrow 2}) + c_{2,i-1} \right) \prod_{j=i}^{k-1} \Gamma_j \right) \\ & + 2\mu\|Y\|_F \left(\|A\|_{2 \rightarrow 2}(c_{1,k-1}\Lambda + c_{2,k-1}\|A\|_{2 \rightarrow 2}) + c_{2,k-1} \right), \end{aligned} \quad (45)$$

where $\{\Gamma_k\}_{k \geq 0}$, $\{c_{1,k}\}_{k \geq 0}$, $\{c_{2,k}\}_{k \geq 0}$ are defined as in Lemma 4.1 and $c_{1,-1} = c_{2,-1} = 0$. In particular, if $\{c_{1,k}\}, \{c_{2,k}\} \leq 1$, then we have the simplified upper bound

$$\|f_W^k(Y)\|_F \leq 2\mu\|Y\|_F (\|A\|_{2 \rightarrow 2}(\Lambda + \|A\|_{2 \rightarrow 2}) + 1)(\zeta_k + 1), \quad (46)$$

where

$$\zeta_k = \frac{\gamma^k - 1}{\gamma - 1} \quad (47)$$

and γ is defined as in Lemma 4.1.

Proof. First, we notice that both $\mathcal{T}(\cdot)$ and $\mathcal{S}(\cdot)$ are 1-Lipschitz functions. Second, by definition of the matrices D_k and Θ_k in (11) and (12) respectively, we have $\|D_k\|_{2 \rightarrow 2} \leq 1$ and $\|\Theta_k\|_{2 \rightarrow 2} = 1$, for any $k \geq 1$, since $0 < \{\theta_k\} \leq 1$ and $\theta_0 = 1$. Now we use the previous statements, along with (17) and (18), to prove (45) via induction. For $k = 1$, we have

$$\begin{aligned} \|f_W^1(Y)\|_F & \leq 2t_0^1\Lambda\|X_0\|_F + 2t_0^2(\|Y\|_F + \|A\|_{2 \rightarrow 2}\|X_0\|_F) \\ & = 2\mu c_{1,0}\Lambda\|A\|_{2 \rightarrow 2}\|Y\|_F + 2\mu c_{2,0}(\|Y\|_F + \|A\|_{2 \rightarrow 2}^2\|Y\|_F) \\ & = 2\mu\|Y\|_F \left(\|A\|_{2 \rightarrow 2}(c_{1,0}\Lambda + c_{2,0}\|A\|_{2 \rightarrow 2}) + c_{2,0} \right). \end{aligned}$$

Suppose (45) holds for k . Then, for $k + 1$:

$$\begin{aligned}
& \|f_W^{k+1}(Y)\|_F < \|f_W^k(Y)\|_F + 2\|G_k^1 f_W^k(Y) - B_k^1\|_F + 2\|G_k^2 f_W^k(Y) - B_k^2\|_F \\
& \leq \|f_W^k(Y)\|_F (2\|G_k^1\|_{2 \rightarrow 2} + 2\|G_k^2\|_{2 \rightarrow 2} + 1) + 2\|B_k^1\|_F + 2\|B_k^2\|_F \\
& \stackrel{\text{Lemma 4.1}}{\leq} \Gamma_k \|f_W^k(Y)\|_F + 2\mu \|X_0\|_F (c_{1,k}\Lambda + c_{2,k}\|A\|_{2 \rightarrow 2}) + 2\mu c_{2,k} \|Y\|_F \\
& \leq \Gamma_k 2\mu \|Y\|_F \sum_{i=0}^{k-1} \left(\left(\|A\|_{2 \rightarrow 2} (c_{1,i-1}\Lambda + c_{2,i-1}\|A\|_{2 \rightarrow 2}) + c_{2,i-1} \right) \prod_{j=i}^{k-1} \Gamma_j \right) \\
& \quad + \Gamma_k 2\mu \|Y\|_F \left(\|A\|_{2 \rightarrow 2} (c_{1,k-1}\Lambda + c_{2,k-1}\|A\|_{2 \rightarrow 2}) + c_{2,k-1} \right) \\
& \quad + 2\mu \|Y\|_F \left(\|A\|_{2 \rightarrow 2} (c_{1,k}\Lambda + c_{2,k}\|A\|_{2 \rightarrow 2}) + c_{2,k} \right) \\
& = 2\mu \|Y\|_F \sum_{i=0}^k \left(\left(\|A\|_{2 \rightarrow 2} (c_{1,i-1}\Lambda + c_{2,i-1}\|A\|_{2 \rightarrow 2}) + c_{2,i-1} \right) \prod_{j=i}^k \Gamma_j \right) \\
& \quad + 2\mu \|Y\|_F \left(\|A\|_{2 \rightarrow 2} (c_{1,k}\Lambda + c_{2,k}\|A\|_{2 \rightarrow 2}) + c_{2,k} \right)
\end{aligned}$$

Therefore, we proved that (45) holds for any $k \in \mathbb{N}$. Now, under the additional assumptions $\{c_{1,k}\}_{k \geq 0}, \{c_{2,k}\}_{k \geq 0} \leq 1$, we may apply Lemma 4.1 on (45), yielding

$$\begin{aligned}
\|f_W^k(Y)\|_F & \leq 2\mu \|Y\|_F \left(\|A\|_{2 \rightarrow 2} (\Lambda + \|A\|_{2 \rightarrow 2}) + 1 \right) \left(\sum_{i=0}^{k-1} \prod_{j=i}^{k-1} \gamma + 1 \right) \\
& = 2\mu \|Y\|_F \left(\|A\|_{2 \rightarrow 2} (\Lambda + \|A\|_{2 \rightarrow 2}) + 1 \right) \left(\sum_{i=1}^k \gamma^i + 1 \right) \\
& = 2\mu \|Y\|_F \left(\|A\|_{2 \rightarrow 2} (\Lambda + \|A\|_{2 \rightarrow 2}) + 1 \right) (\zeta_k + 1),
\end{aligned}$$

where

$$\zeta_k = \frac{\gamma^k - 1}{\gamma - 1} \quad (48)$$

and γ is defined as in Lemma 4.1. \square

4.2 Lipschitzness results

We state our first important Theorem, regarding the Lipschitz continuity of the intermediate decoder defined in (21). Its proof can be found at Appendix A.

Theorem 4.3. *Let f_W^L defined as in (21), $L \geq 2$, dictionary $W \in \mathcal{B}_\Lambda$, step sizes $\{t_k^1\}_{k \geq -1}, \{t_k^2\}_{k \geq -1} > 0$ with $t_0^1 = t_0^2 = 1, t_{-1}^1 = t_{-1}^2 = 0$, step size multiplier $0 < \{\theta_k\}_{k \geq -1} \leq 1$ with $\theta_0 = \theta_{-1} = 1$, and smoothing parameter $\mu > 0$. Then, for any $W_1, W_2 \in \mathcal{B}_\Lambda$, we have*

$$\|f_{W_1}^L(Y) - f_{W_2}^L(Y)\|_F \leq K_L \|W_1 - W_2\|_{2 \rightarrow 2}, \quad (49)$$

where

$$\begin{aligned}
K_L = & 2\mu\|Y\|_F \left[\mu^{-1}\|A\|_{2 \rightarrow 2} + \sum_{k=2}^L \left(\left(\max_{0 \leq l \leq L-1} \Gamma_l \right)^{L-k} 2 \left[\sum_{i=0}^{k-2} \left(\|A\|_{2 \rightarrow 2} \right. \right. \right. \\
& \cdot (c_{1,i-1}\Lambda + c_{2,i-1}\|A\|_{2 \rightarrow 2}) + c_{2,i-1} \left. \left. \left. \prod_{j=i}^{k-2} \Gamma_j \right) \right. \right. \\
& + \left. \left. \left. \left(\|A\|_{2 \rightarrow 2}(c_{1,k-2}\Lambda + c_{2,k-2}\|A\|_{2 \rightarrow 2}) + c_{2,k-2} \right) \right. \right. \\
& \cdot \left. \left. \left. \left(2\Lambda c_{1,k-1} + \|A\|_{2 \rightarrow 2}(c_{1,k-1} + c_{2,k-1}) \right) + c_{1,k-1}\|A\|_{2 \rightarrow 2} \right) \right] \right], \tag{50}
\end{aligned}$$

with $\{\Gamma_k\}_{k \geq 0}$, $\{c_{1,k}\}_{k \geq 0}$, $\{c_{2,k}\}_{k \geq 0}$ defined as in Lemma 4.1 and $c_{1,-1} = c_{2,-1} = 0$. Moreover, if $\{c_{1,k}\}, \{c_{2,k}\} \leq 1$, then we have the simplified upper bound

$$\begin{aligned}
K_L < & 2\mu\|Y\|_F \left[\|A\|_{2 \rightarrow 2}(\mu^{-1} + (L-1)) \right. \\
& \left. + 4\|A\|_{2 \rightarrow 2}((\Lambda + \|A\|_{2 \rightarrow 2}) + 1)(\Lambda + \|A\|_{2 \rightarrow 2})\kappa_L \right], \tag{51}
\end{aligned}$$

with

$$\kappa_L = \frac{\gamma^L((L-2) + \gamma^2(\gamma-2)) - \gamma^2(\gamma-2)}{\gamma-1} \tag{52}$$

and γ as in Lemma 4.1.

It is time to prove the Lipschitzness of the decoder defined in (25).

Corollary 4.4. *Let $h \in \mathcal{H}^L$ defined as in (26) with $L \geq 2$ and dictionary $W \in \mathcal{B}_\Lambda$. Then, for any $W_1, W_2 \in \mathcal{B}_\Lambda$, we have:*

$$\|\psi(\phi(f_{W_2}^L(Y))) - \psi(\phi(f_{W_1}^L(Y)))\|_F \leq \mu^{-1}(\Lambda + \|A\|_{2 \rightarrow 2})K_L\|W_2 - W_1\|_F, \tag{53}$$

with K_L as in Theorem 4.3.

Proof. By definition, ψ is a 1-Lipschitz function. Moreover, as an affine map, ϕ is Lipschitz continuous with Lipschitz constant $\text{Lip}_\phi = \|\Phi\|_{2 \rightarrow 2}$, where Φ is defined in (23). We evaluate $\|\Phi\|_{2 \rightarrow 2}$:

$$\begin{aligned}
\|\Phi\|_{2 \rightarrow 2} & \leq \mu^{-1}\theta_L\|W\|_{2 \rightarrow 2} + \mu^{-1}\theta_L\|A\|_{2 \rightarrow 2} + \mu^{-1}(1 - \theta_L)\|W\|_{2 \rightarrow 2} \\
& \quad + \mu^{-1}(1 - \theta_L)\|A\|_{2 \rightarrow 2} \leq \mu^{-1}(\Lambda + \|A\|_{2 \rightarrow 2}).
\end{aligned}$$

Combining the previous estimates, we get

$$\begin{aligned}
& \|\psi(\phi(f_{W_2}^L(Y))) - \psi(\phi(f_{W_1}^L(Y)))\|_F \leq \|\phi(f_{W_2}^L(Y)) - \phi(f_{W_1}^L(Y))\|_F \\
& \leq \|\Phi\|_{2 \rightarrow 2}\|f_{W_2}^L(Y) - f_{W_1}^L(Y)\|_F \leq \mu^{-1}(\Lambda + \|A\|_{2 \rightarrow 2})K_L\|W_2 - W_1\|_F,
\end{aligned}$$

where in the last inequality we used Theorem 4.3. \square

5 Main Results

In this Section, we estimate the desired generalization error. To do so, we combine the tools we developed so far with a chaining technique.

5.1 Covering numbers and Dudley's inequality

For a fixed number of layers $L \in \mathbb{N}$, we define the set $\mathcal{M} \subset \mathbb{R}^{n \times s}$ corresponding to the hypothesis class \mathcal{H}^L :

$$\begin{aligned} \mathcal{M} &:= \{(h(y_1)|h(y_2)|\dots|h(y_s)) \in \mathbb{R}^{n \times s} : h \in \mathcal{H}^L\} \\ &= \{\psi(\phi((f_W^L(Y))) \in \mathbb{R}^{n \times s} : W \in \mathcal{B}_\Lambda\}. \end{aligned} \quad (54)$$

The column elements of each matrix in \mathcal{M} are the reconstructions given by a decoder $h \in \mathcal{H}^L$ when applied to the measurements y_i . Since \mathcal{M} is parameterized by W like \mathcal{H}^L is, we may rewrite (37) as

$$\begin{aligned} \mathcal{R}_s(l \circ \mathcal{H}^L) &\leq \sqrt{2}(2B_{\text{in}} + 2B_{\text{out}})\mathcal{R}_s(\mathcal{H}^L) = \sqrt{2}(2B_{\text{in}} + 2B_{\text{out}})\mathcal{R}_s(\mathcal{M}) \\ &= \sqrt{2}(2B_{\text{in}} + 2B_{\text{out}})\mathbb{E} \sup_{M \in \mathcal{M}} \frac{1}{s} \sum_{i=1}^s \sum_{k=1}^n \epsilon_{ik} M_{ik}. \end{aligned} \quad (55)$$

Thus, we are left with estimating the Rademacher process

$$\mathbb{E} \sup_{M \in \mathcal{M}} \frac{1}{s} \sum_{i=1}^s \sum_{k=1}^n \epsilon_{ik} M_{ik}. \quad (56)$$

The latter has subgaussian increments, hence we use Dudley's inequality [38] to upper bound it in terms of the covering numbers of the set \mathcal{M} .

Theorem 5.1 (Dudley's inequality). *Let $(X_t)_{t \in T}$ be a centered subgaussian process with radius $\Delta(T) = \sup_{t \in T} \sqrt{\mathbb{E}|X_t|^2}$. Then,*

$$\mathbb{E} \sup_{t \in T} X_t \leq 4\sqrt{2} \int_0^{\Delta(T)/2} \sqrt{\log(\mathcal{N}(T, d, u))} du. \quad (57)$$

Therefore, we first calculate the radius of \mathcal{M} , i.e.

$$\begin{aligned} \Delta(\mathcal{M}) &= \sup_{h \in \mathcal{H}^L} \sqrt{\mathbb{E} \left(\sum_{i=1}^s \sum_{k=1}^n \epsilon_{ik} h_k(y_i) \right)^2} \leq \sup_{h \in \mathcal{H}^L} \sqrt{\mathbb{E} \sum_{i=1}^s \sum_{k=1}^n \epsilon_{ik} (h_k(y_i))^2} \\ &\leq \sup_{h \in \mathcal{H}^L} \sqrt{\sum_{i=1}^s \|h(y_i)\|_2^2} \stackrel{(39)}{\leq} \sqrt{s} B_{\text{out}}. \end{aligned} \quad (58)$$

Now, applying Theorem 5.1 to (55) yields

$$\mathcal{R}_s(l \circ \mathcal{H}^L) \leq \frac{16(B_{\text{in}} + B_{\text{out}})}{s} \int_0^{\sqrt{s} B_{\text{out}}/2} \sqrt{\log \mathcal{N}(\mathcal{M}, \|\cdot\|_F, \varepsilon)} d\varepsilon. \quad (59)$$

According to (59), we need to estimate $\mathcal{N}(\mathcal{M}, \|\cdot\|_F, \varepsilon)$. Towards that end, we state the following Lemma.

Lemma 5.2. *The covering number of $B_{\|\cdot\|_{2 \rightarrow 2}}^{N \times n}(\Lambda) = \{X \in \mathbb{R}^{N \times n} : \|X\|_{2 \rightarrow 2} \leq \Lambda, \Lambda > 0\}$ satisfies the following for any $\varepsilon > 0$:*

$$\mathcal{N}(B_{\|\cdot\|_{2 \rightarrow 2}}^{N \times n}(\Lambda), \|\cdot\|_{2 \rightarrow 2}, \varepsilon) \leq \left(1 + \frac{2\Lambda}{\varepsilon}\right)^{Nn}. \quad (60)$$

Proof. For $|\cdot|$ denoting the volume in $\mathbb{R}^{N \times n}$, the following is an adaptation of a well-known result (Proposition 4.2.12 of [50]) connecting covering numbers and volume in $\mathbb{R}^{N \times n}$:

$$\begin{aligned} \mathcal{N}(B_{\|\cdot\|_{2 \rightarrow 2}}^{N \times n}(\Lambda), \|\cdot\|_{2 \rightarrow 2}, \varepsilon) &\leq \frac{|B_{\|\cdot\|_{2 \rightarrow 2}}^{N \times n}(\Lambda) + (\varepsilon/2)B_{\|\cdot\|_{2 \rightarrow 2}}^{N \times n}(1)|}{|(\varepsilon/2)B_{\|\cdot\|_{2 \rightarrow 2}}^{N \times n}(1)|} \\ &= \frac{|\Lambda \cdot B_{\|\cdot\|_{2 \rightarrow 2}}^{N \times n}(1) + (\varepsilon/2)B_{\|\cdot\|_{2 \rightarrow 2}}^{N \times n}(1)|}{|(\varepsilon/2)B_{\|\cdot\|_{2 \rightarrow 2}}^{N \times n}(1)|} \\ &= \frac{|(\Lambda + \varepsilon/2)B_{\|\cdot\|_{2 \rightarrow 2}}^{N \times n}(1)|}{|(\varepsilon/2)B_{\|\cdot\|_{2 \rightarrow 2}}^{N \times n}(1)|}. \end{aligned}$$

Hence,

$$\mathcal{N}(B_{\|\cdot\|_{2 \rightarrow 2}}^{N \times n}(\Lambda), \|\cdot\|_{2 \rightarrow 2}, \varepsilon) \leq \left(1 + \frac{2\Lambda}{\varepsilon}\right)^{Nn}. \quad \square$$

Proposition 5.3. *The following estimate holds for the covering numbers of \mathcal{M} :*

$$\mathcal{N}(\mathcal{M}, \|\cdot\|_F, \varepsilon) \leq \left(1 + \frac{2\Lambda\mu^{-1}(\Lambda + \|A\|_{2 \rightarrow 2})K_L}{\varepsilon}\right)^{Nn}. \quad (61)$$

Proof. We first consider the set $\Omega = \{W : W \in \mathcal{B}_\Lambda\} \subset \mathbb{R}^{N \times n}$. Then, due to Lemma 5.2, we can upper bound the covering numbers of Ω as follows:

$$\mathcal{N}(\Omega, \|\cdot\|_{2 \rightarrow 2}, \varepsilon) \leq \left(1 + \frac{2\Lambda}{\varepsilon}\right)^{Nn}. \quad (62)$$

Now, for the covering numbers of \mathcal{M} we have

$$\begin{aligned} \mathcal{N}(\mathcal{M}, \|\cdot\|_F, \varepsilon) &\leq \mathcal{N}(\mu^{-1}(\Lambda + \|A\|_{2 \rightarrow 2})K_L\Omega, \|\cdot\|_{2 \rightarrow 2}, \varepsilon) \\ &= \mathcal{N}(\Omega, \|\cdot\|_{2 \rightarrow 2}, \varepsilon/(\mu^{-1}(\Lambda + \|A\|_{2 \rightarrow 2})K_L)) \\ &\leq \left(1 + \frac{2\Lambda\mu^{-1}(\Lambda + \|A\|_{2 \rightarrow 2})K_L}{\varepsilon}\right)^{Nn}. \quad \square \end{aligned}$$

5.2 Generalization error bounds for DECONET

We are now in position to prove our main results, that estimate the generalization error of DECONET.

Theorem 5.4. *Let \mathcal{H}^L be the hypothesis class defined in (26). With probability at least $1 - \delta$, for all $h \in \mathcal{H}^L$, the generalization error is bounded as*

$$\begin{aligned} \mathcal{L}(h) &\leq \hat{\mathcal{L}}(h) + 8(B_{\text{in}} + B_{\text{out}})B_{\text{out}} \sqrt{\frac{Nn}{s}} \sqrt{\log \left(e \left(1 + \frac{4\mu^{-1}\Lambda(\Lambda + \|A\|_{2 \rightarrow 2})K_L}{\sqrt{s}B_{\text{out}}} \right) \right)} \\ &\quad + 4(B_{\text{in}} + B_{\text{out}})^2 \sqrt{\frac{2 \log(4/\delta)}{s}}, \end{aligned} \quad (63)$$

with K_L defined in (50).

Proof. We apply Proposition 5.3 to (59), yielding:

$$\begin{aligned} \mathcal{R}_s(l \circ \mathcal{H}^L) &\leq \frac{16(B_{\text{in}} + B_{\text{out}})}{s} \int_0^{\frac{\sqrt{s}B_{\text{out}}}{2}} \sqrt{\log \mathcal{N}(\mathcal{M}, \|\cdot\|_F, \varepsilon)} d\varepsilon \\ &\leq \frac{16(B_{\text{in}} + B_{\text{out}})}{s} \int_0^{\frac{\sqrt{s}B_{\text{out}}}{2}} \sqrt{Nn \log \left(1 + \frac{2\Lambda\mu^{-1}(\Lambda + \|A\|_{2 \rightarrow 2})K_L}{\varepsilon} \right)} d\varepsilon \\ &\leq 8(B_{\text{in}} + B_{\text{out}})B_{\text{out}} \sqrt{\frac{Nn}{s}} \sqrt{\log \left(e \left(1 + \frac{4\Lambda\mu^{-1}(\Lambda + \|A\|_{2 \rightarrow 2})K_L}{\sqrt{s}B_{\text{out}}} \right) \right)}, \end{aligned}$$

where in the last step we used the inequality

$$\int_0^a \sqrt{\log \left(1 + \frac{b}{t} \right)} dt \leq a \sqrt{\log(e(1 + b/a))}, \quad a, b > 0.$$

Now, we use Theorem 3.1 with the upper bound $c = (B_{\text{in}} + B_{\text{out}})^2$ for the loss function $\|\cdot\|_2^2$, and the proof follows. \square

Similarly to Section 4, we may further assume that the ratios $\{t_k^1/\mu\theta_k\}_{k \geq 0}$, $\{t_k^2/\mu\theta_k\}_{k \geq 0}$ are upper bounded by 1, so we obtain

Corollary 5.5. *Let \mathcal{H}^L be the hypothesis class defined in (26) and assume that $\{t_k^1/\mu\theta_k\}_{k \geq 0}$, $\{t_k^2/\mu\theta_k\}_{k \geq 0} \leq 1$. With probability at least $1 - \delta$, for all $h \in \mathcal{H}^L$, the generalization error is bounded as*

$$\begin{aligned} \mathcal{L}(h) &< \hat{\mathcal{L}}(h) + 8(B_{\text{in}} + B_{\text{out}}) \left(B_{\text{out}} \sqrt{\frac{Nn}{s}} \right. \\ &\quad \left. \cdot \sqrt{\log \left(e \left(1 + \frac{\|Y\|_F(p + q(L-1)) + r\kappa_L}{\sqrt{s}B_{\text{out}}} \right) \right)} + \sqrt{\frac{2 \log(4/\delta)}{s}} \right), \end{aligned} \quad (64)$$

with κ_L as in Theorem 4.3 and $p, q, r > 0$ constants depending on $\|A\|_{2 \rightarrow 2}, \Lambda, \mu$.

Proof. The estimate easily follows from Theorems 4.3 - 5.4, if we set

$$p := 8\mu^{-1}\Lambda(\Lambda + \|A\|_{2 \rightarrow 2})\|A\|_{2 \rightarrow 2} \quad (65)$$

$$q := 8\Lambda(\Lambda + \|A\|_{2 \rightarrow 2}) \quad (66)$$

$$r := 32\Lambda(\Lambda + \|A\|_{2 \rightarrow 2})\|A\|_{2 \rightarrow 2}((\Lambda + \|A\|_{2 \rightarrow 2}) + 1)(\Lambda + \|A\|_{2 \rightarrow 2}). \quad (67)$$

□

All the previous results are now summarized in

Theorem 5.6. *Let \mathcal{H}^L be the hypothesis class defined in (26). Assume there exist pair-samples $\{(x_i, y_i)\}_{i=1}^s$, with $y_i = Ax_i + e$, $\|e\|_2 \leq \varepsilon$, for some $\varepsilon > 0$, that are drawn i.i.d. according to an unknown distribution \mathcal{D} , and that it holds $\|y_i\|_2 \leq B_{\text{in}}$ almost surely with $B_{\text{in}} = B_{\text{out}}$ in (24). Let us further assume that for step sizes $\{t_k^1\}_{k \geq 0}$, $\{t_k^2\}_{k \geq 0} > 0$, step size multiplier $0 < \{\theta_k\}_{k \geq 0} \leq 1$ and smoothing parameter $\mu > 0$, we have $\{t_k^1/\mu\theta_k\}_{k \geq 0}$, $\{t_k^2/\mu\theta_k\}_{k \geq 0} \leq 1$. Then with probability at least $1 - \delta$, for all $h \in \mathcal{H}^L$, the generalization error is bounded as*

$$\begin{aligned} \mathcal{L}(h) &< \hat{\mathcal{L}}(h) + 16B_{\text{out}}^2 \sqrt{\frac{Nn}{s}} \sqrt{\log(e(1+p+q(L-1)) + r\kappa_L)} \\ &+ 16B_{\text{out}} \sqrt{\frac{2 \log(4/\delta)}{s}}. \end{aligned} \quad (68)$$

We also state below a key remark, regarding the generalization error bound as a function of L, N and s .

Remark 5.7. *According to (52), we have that L enters at most exponentially in the definition of κ_L . Now, if we consider the dependence of the generalization error bound (68) only on L, N, s and treat all other terms as constants, we roughly have*

$$|\mathcal{L}(h) - \hat{\mathcal{L}}(h)| \lesssim \sqrt{\frac{NL}{s}}. \quad (69)$$

6 Numerical Experiments

In this Section, we are interested in examining whether our theory regarding the generalization error of DECONET is consistent with real-world CS paradigms.

6.1 Settings

We train and test DECONET on two real-world image datasets: MNIST (60000 training and 10000 test 28×28 image examples) and CIFAR10 [51] (50000 training and 10000 test 32×32 coloured image examples). For the CIFAR10 dataset, we transform the images into grayscale ones. For both datasets, we consider the vectorized form of the images. We examine DECONET with varying number of layers L . We consider two CS ratios, i.e. $m/n = 25\%$ and $m/n = 50\%$.

We choose a random Gaussian measurement matrix $A \in \mathbb{R}^{m \times n}$ and appropriately normalize it, i.e., $\tilde{A} = A/\sqrt{m}$. We add zero-mean Gaussian noise e with standard deviation $\text{std} = 10^{-4}$ to the measurements y , so that $y = \tilde{A}x + e$. We set $\varepsilon = \|y - \tilde{A}x\|_2$ and $x_0 = A^T y$, which are standard algorithmic setups. We take different values of N and perform He (normal) initialization for $W \in \mathbb{R}^{N \times n}$. We set $\mu = 100$, initial step sizes $t_0^1 = t_0^2 = 1$ and step size multiplier $\theta_0 = 1$. The authors in [37] define $t_k^2 = \alpha t_k^1$, where $\alpha = \frac{\|W\|_2^2}{\|A\|_2^2}$, but in the current we extend their result by adapting separately t_k^1, t_k^2 , with $t_k^1 = \alpha t_{k-1}^1$, $t_k^2 = \beta t_{k-1}^2$, $k = 1, \dots, L$, respectively, where $(\alpha, \beta) \in (0, 1) \times (0, 1)$. We set $(\alpha, \beta) = (0.5, 0.3)$ and $(\alpha, \beta) = (0.7, 0.5)$ for the MNIST and CIFAR10 datasets, respectively. Moreover, we consider the following update rule for the step size multiplier: $\theta_k = \theta_{k-1} \cdot \theta_s$, $k = 1, \dots, L$, where $\theta_s = \frac{1 - \sqrt{\mu/\tilde{L}}}{1 + \sqrt{\mu/\tilde{L}}}$ and \tilde{L} is an upper bound on the smoothing parameter μ ; we set $\tilde{L} = 1000$. For MNIST and CIFAR10, we train all networks with learning rate $\eta = 10^{-2}$ and $\eta = 10^{-3}$, respectively. All networks are implemented in PyTorch [52] and trained using the *Adam* optimizer [53], with batch size 128. For our experiments, we report the *test MSE* defined by

$$\mathcal{L}_{test} = \frac{1}{d} \sum_{i=1}^d \|h(\tilde{y}_i) - \tilde{x}_i\|_2^2, \quad (70)$$

where $\mathcal{D} = \{(\tilde{y}_i, \tilde{x}_i)\}_{i=1}^d$ is a set of d test data, not used in the training phase, and the *empirical generalization error* (EGE) defined by

$$\mathcal{L}_{gen} = |\mathcal{L}_{test} - \mathcal{L}_{train}|, \quad (71)$$

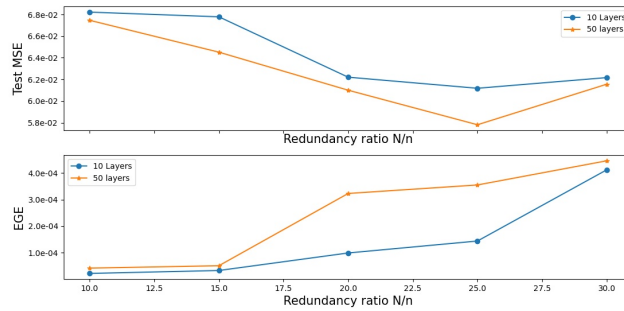
where \mathcal{L}_{train} is the train MSE defined in (28). Due to the fact that test MSE approximates the true loss, we use (71) – which can be explicitly computed – to approximate (30). We train all networks, on all datasets, employing an early stopping technique [54] with respect to (71). We repeat all the experiments at least 10 times and average the results over the runs. Finally, we compare the EGE of DECONET to the EGE achieved by the state-of-the-art ISTA-net, proposed in [21]; the latter jointly learns a decoder for CS and an orthogonal dictionary for sparsification. Under this setting, ISTA-net solves the CS problem employing synthesis sparsity, while DECONET solves the analysis-sparsity-based CS. We aim to see how the EGE is affected by each of the two sparsity models. For ISTA-net, we set the best hyper-parameters proposed by the original authors.

6.2 Experiments

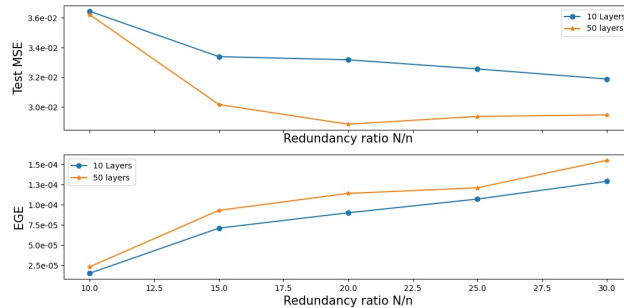
We test DECONET on MNIST and CIFAR10 datasets under multiple experimental scenarios.

6.2.1 Fixed CS ratio for 10- and 50-layer DECONET with varying N/n

We examine the performance of 10- and 50-layer DECONET for a fixed 25% CS ratio, redundancy ratio N/n varying in the set $\{10, 15, 20, 25, 30\}$ and report the results in Fig. 1a (MNIST) and 1b (CIFAR10). The top subplots of Fig. 1a and 1b illustrate how the test MSEs, achieved by 10- and 50-layer DECONET, drop as L and N/n increase. The decays seem reasonable, if one considers a standard analysis CS scenario: a) the performance and reconstruction quality provided by the analysis- l_1 algorithm typically benefit from the (high) redundancy offered by the involved analysis operator b) more iterations/layers result to a higher reconstruction quality. The bottom subplots of Fig. 1a and 1b demonstrate the increment of the EGEs, achieved by 10- and 50-layer DECONET, as both L and N/n increase. This behaviour confirms our theoretical result depicted in Theorem 5.6 (and Remark 5.7).



(a) MNIST



(b) CIFAR10

Figure 1: Average test MSEs (top subplots) and empirical generalization errors (bottom subplots) for 10- and 50-layer DECONET, with 25% CS ratio, tested on (a) MNIST and (b) CIFAR10 datasets.

6.2.2 Fixed CS ratio with varying L and N

We examine the generalization ability of DECONET for $m = n/2$, with increasing number of layers L , under different choices of N . Inspired by frames with redundancy ratio $N/n \notin \mathbb{N}$ [55], we consider N of the form

$$N = pn^2 + q, \quad p, q \in \mathbb{N}. \quad (72)$$

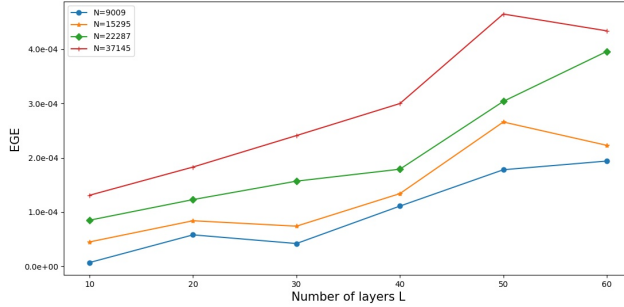
We report the results in Fig. 2a (MNIST) and 2b (CIFAR10). Similarly to Section 6.2.1, we observe that the empirical generalization error increases in L and N , for both datasets. Even though the upper bound in (68) depends on many terms, the empirical generalization error appears to grow at the rate of \sqrt{N} . The behaviour of DECONET again conforms with our theoretical results presented in Theorem 5.6. One may also notice that – in general – we choose different N for each of the two datasets; this is simply due to (72), i.e., N depends on the vectorized ambient dimension n , which is different for each of the two datasets.

6.2.3 DECONET vs ISTA-net

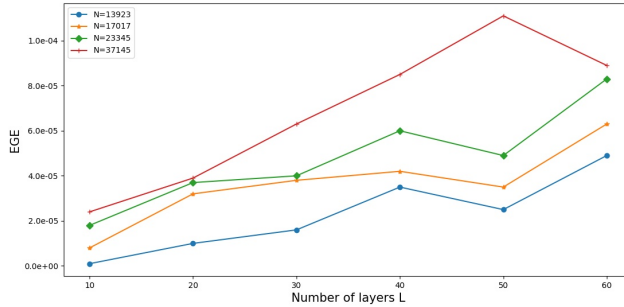
In this set of experiments, we aim to see how analysis and synthesis sparsity models affect the generalization ability of CS-oriented unfolding networks. Towards this end, we compare the proposed DECONET’s decoder to ISTA-net’s decoder, for 10, 30 and 50 layers, with 25% and 50% CS ratio, and fixed $N = 37145$ for our learnable analysis operator, on all datasets. We report the corresponding empirical generalization errors in Table 1. First of all, we see that our proposed decoder outperforms the ISTA-net’s decoder, consistently for both datasets. This behaviour indicates that learning a redundant sparsifier instead of an orthogonal one, improves the performance of a CS-oriented unfolding network. Second, our theoretical result seems to align with the experiments, since the EGE of DECONET increases as L also increases. Moreover, for the CIFAR10 dataset, the EGE of DECONET decreases as the number of measurements m increases, but this decay is not explained by our theoretical result, which does not account for m . Hence, this observation is in need of future mathematical explanation.

7 Conclusion and Future Work

In the present paper we derived DECONET, a new deep unfolding network for solving the analysis-sparsity-based Compressed Sensing problem, by unfolding the iterations of a state-of-the-art optimization algorithm into layers of the network. DECONET jointly learns a CS decoder and a redundant analysis operator, serving as a sparsifying transform. We introduced the hypothesis class consisting of all the functions/decoders that DECONET can implement and upper bounded its corresponding Rademacher complexity using chaining techniques. In the end, we derived generalization error bounds for DECONET, in



(a) Empirical generalization error for $m = n/2$ measurements on MNIST, with alternating N



(b) Empirical generalization error for $m = n/2$ measurements on CIFAR10, with alternating N

Figure 2: Performance plots for DECONET with 50% CS ratio, tested on MNIST (top) and CIFAR10 (bottom) datasets.

| | | 25% CS ratio | | | | | |
|---------|----------|-----------------|-----------------|-----------------|-----------------|-----------------|------------------|
| Dataset | | MNIST | | | CIFAR10 | | |
| Layers | | $L = 10$ | $L = 30$ | $L = 50$ | $L = 10$ | $L = 30$ | $L = 50$ |
| Decoder | DECONET | 0.000033 | 0.000314 | 0.000446 | 0.000066 | 0.000100 | 0.0000128 |
| Decoder | ISTA-net | 0.013408 | 0.007874 | 0.005937 | 0.007165 | 0.004120 | 0.003085 |

| | | 50% CS ratio | | | | | |
|---------|----------|-----------------|-----------------|-----------------|-----------------|-----------------|-----------------|
| Dataset | | MNIST | | | CIFAR10 | | |
| Layers | | $L = 10$ | $L = 30$ | $L = 50$ | $L = 10$ | $L = 30$ | $L = 50$ |
| Decoder | DECONET | 0.000131 | 0.000241 | 0.000465 | 0.000024 | 0.000063 | 0.000111 |
| Decoder | ISTA-net | 0.016547 | 0.009311 | 0.007157 | 0.009274 | 0.005576 | 0.004377 |

Table 1: Empirical generalization error for 10-, 30- and 50-layer decoders (all datasets), with fixed $N = 37145$. Bold letters indicate the best performance between the two decoders.

terms of the aforementioned Rademacher complexity estimate. Our generalization error bounds roughly scale like the square root of the number of layers and the redundancy of the learned analysis operator. To the best of our knowledge, this is the first result of its kind for unfolding networks solving the analysis CS problem. Furthermore, we conducted experiments that confirmed the validity of our derived theory and compared DECONET to a state-of-the-art learnable synthesis-sparsity-based decoder; the former outperformed the latter in terms of generalization error. This behaviour confirms improved performance when learning a redundant sparsifier for CS instead of an orthogonal one. As a future direction, we could also learn some of the parameters of the original iterative algorithm. Furthermore, it would be interesting to check if the redundancy of the learnable sparsifier introduces some kind of implicit regularization into DECONET.

Acknowledgements

The author would like to thank H. Rauhut for his valuable advice and inspiring conversations around the subject covered in this paper.

Appendix A

We state here the proof of Theorem 4.3.

Proof. First, we set $f_{W_1}^0(Y) = f_{W_2}^0(Y) = Y$ for a uniform treatment of all layers. Then, we write $\{G_{1,k}^i\}_{i=1,2}$, $\{G_{2,k}^i\}_{i=1,2}$ (similarly for $\{B_{1,k}^i\}_{i=1,2}$, $\{B_{2,k}^i\}_{i=1,2}$) to denote the dependency on W_1, W_2 , respectively. By the 1-Lipschitzness of $\mathcal{T}(\cdot), \mathcal{S}(\cdot)$, the estimates $\|D_k\|_{2 \rightarrow 2} \leq 1$ and $\|\Theta_k\|_{2 \rightarrow 2} = 1$ that hold for any

$k \geq 0$, and the introduction of mixed terms, we get

$$\begin{aligned}
& \|f_{W_1}^k(Y) - f_{W_2}^k(Y)\|_F \\
& \leq \|D_{k-1}f_{W_1}^{k-1}(Y) + \Theta_{k-1}\sigma(f_{W_1}^{k-1}) - D_{k-1}f_{W_2}^{k-1}(Y) - \Theta_{k-1}\sigma(f_{W_2}^{k-1})\|_F \\
& \leq \|D_{k-1}\|_{2 \rightarrow 2} \|f_{W_1}^{k-1}(Y) - f_{W_2}^{k-1}(Y)\|_F + \|\Theta_{k-1}\|_{2 \rightarrow 2} \|\sigma(f_{W_1}^{k-1}) - \sigma(f_{W_2}^{k-1})\|_F \\
& \leq \|f_{W_1}^{k-1}(Y) - f_{W_2}^{k-1}(Y)\|_F + 2\|G_{1,k-1}^1 f_{W_1}^{k-1}(Y) - B_{1,k-1}^1 - G_{2,k-1}^1 f_{W_2}^{k-1}(Y) \\
& \quad + B_{2,k-1}^1\|_F + 2\|G_{1,k-1}^2 f_{W_1}^{k-1}(Y) - B_{1,k-1}^2 - G_{2,k-1}^2 f_{W_2}^{k-1}(Y) + B_{2,k-1}^2\|_F \\
& = \|f_{W_1}^{k-1}(Y) - f_{W_2}^{k-1}(Y)\|_F + 2\|G_{1,k-1}^1 f_{W_1}^{k-1}(Y) - B_{1,k-1}^1 + G_{1,k-1}^1 f_{W_2}^{k-1}(Y) \\
& \quad - G_{1,k-1}^1 f_{W_2}^{k-1}(Y) - G_{2,k-1}^1 f_{W_2}^{k-1}(Y) + B_{2,k-1}^1\|_F + 2\|G_{1,k-1}^2 f_{W_1}^{k-1}(Y) - B_{1,k-1}^2 \\
& \quad + G_{1,k-1}^2 f_{W_2}^{k-1}(Y) - G_{2,k-1}^2 f_{W_2}^{k-1}(Y) - G_{2,k-1}^2 f_{W_2}^{k-1}(Y) + B_{2,k-1}^2\|_F \\
& \leq \|f_{W_1}^{k-1}(Y) - f_{W_2}^{k-1}(Y)\|_F + 2(\|G_{1,k-1}^1\|_{2 \rightarrow 2} \|f_{W_1}^{k-1}(Y) - f_{W_2}^{k-1}(Y)\|_F \\
& \quad + \|f_{W_2}^{k-1}(Y)\|_F \|G_{2,k-1}^1 - G_{1,k-1}^1\|_{2 \rightarrow 2} + \|B_{2,k-1}^1 - B_{1,k-1}^1\|_F) \\
& + 2(\|G_{1,k-1}^2\|_{2 \rightarrow 2} \|f_{W_1}^{k-1}(Y) - f_{W_2}^{k-1}(Y)\|_F + \|f_{W_2}^{k-1}(Y)\|_F \|G_{2,k-1}^2 - G_{1,k-1}^2\|_{2 \rightarrow 2} \\
& \quad + \underbrace{\|B_{2,k-1}^2 - B_{1,k-1}^2\|_F}_{=0, \text{ since it is not parameter-dependent}}),
\end{aligned}$$

Consequently,

$$\begin{aligned}
& \|f_{W_1}^k(Y) - f_{W_2}^k(Y)\|_F \leq \|f_{W_1}^{k-1}(Y) - f_{W_2}^{k-1}(Y)\|_F (2\|G_{1,k-1}^1\|_{2 \rightarrow 2} \\
& \quad + 2\|G_{1,k-1}^2\|_{2 \rightarrow 2} + 1) + 2\|f_{W_2}^{k-1}(Y)\|_F (\|G_{1,k-1}^2 - G_{2,k-1}^2\|_{2 \rightarrow 2} \\
& \quad + \|G_{1,k-1}^1 - G_{2,k-1}^1\|_{2 \rightarrow 2}) + 2\|B_{2,k-1}^1 - B_{1,k-1}^1\|_F.
\end{aligned} \tag{73}$$

For simplification, we will treat separately some terms in (73).

Estimation of $2\|G_{1,k-1}^1\|_{2 \rightarrow 2} + 2\|G_{1,k-1}^2\|_{2 \rightarrow 2} + 1$. Due to Lemma 4.1 and the assumption that $W_1, W_2 \in \mathcal{B}_\Lambda$, we have

$$2\|G_{1,k-1}^1\|_{2 \rightarrow 2} + 2\|G_{1,k-1}^2\|_{2 \rightarrow 2} + 1 \leq \Gamma_{k-1}, \tag{74}$$

with $\{\Gamma_k\}_{k \geq 0}$ defined as in Lemma 4.1.

Estimation of $\|G_{2,k-1}^1 - G_{1,k-1}^1\|_{2 \rightarrow 2} + \|G_{2,k-1}^2 - G_{1,k-1}^2\|_{2 \rightarrow 2}$.

$$\begin{aligned}
& \|G_{2,k-1}^1 - G_{1,k-1}^1\|_{2 \rightarrow 2} + \|G_{2,k-1}^2 - G_{1,k-1}^2\|_{2 \rightarrow 2} \\
& \leq [\mu^{-1}t_{k-1}^1 \|W_2 W_2^T - W_1 W_1^T\|_{2 \rightarrow 2} + \mu^{-1}t_{k-1}^1 \|A\|_{2 \rightarrow 2} \|W_2 - W_1\|_{2 \rightarrow 2} \\
& \quad + (1 - \theta_{k-1})\theta_{k-1}^{-1} \mu^{-1}t_{k-1}^1 \|W_2 W_2^T - W_1 W_1^T\|_{2 \rightarrow 2} \\
& \quad + (1 - \theta_{k-1})\theta_{k-1}^{-1} \mu^{-1}t_{k-1}^1 \|A\|_{2 \rightarrow 2} \|W_2 - W_1\|_{2 \rightarrow 2}] \\
& \quad + [\mu^{-1}t_{k-1}^2 \|A\|_{2 \rightarrow 2} \|W_2 - W_1\|_{2 \rightarrow 2} \\
& \quad + (1 - \theta_{k-1})\theta_{k-1}^{-1} \mu^{-1}t_{k-1}^2 \|A\|_{2 \rightarrow 2} \|W_2 - W_1\|_{2 \rightarrow 2}]
\end{aligned} \tag{75}$$

We define $c_{1,k} = \theta_k^{-1} \mu^{-1} t_k^1$, $c_{2,k} = \theta_k^{-1} \mu^{-1} t_k^2$, for $k \geq -1$, and $c_{1,-1} = c_{2,-1} = 0$ (this holds due to the assumption that $t_{-1}^1 = t_{-1}^2 = 0$). The previous statements and the assumption that $0 < \{\theta_k\}_{k \geq -1} \leq 1$, yield for (75)

$$\begin{aligned} & \|G_{2,k-1}^1 - G_{1,k-1}^1\|_{2 \rightarrow 2} + \|G_{2,k-1}^2 - G_{1,k-1}^2\|_{2 \rightarrow 2} \\ & \leq c_{1,k-1} \|W_2 W_2^T - W_1 W_1^T\|_{2 \rightarrow 2} + \|A\|_{2 \rightarrow 2} \|W_2 - W_1\|_{2 \rightarrow 2} (c_{1,k-1} + c_{2,k-1}). \end{aligned} \quad (76)$$

Furthermore,

$$\begin{aligned} \|W_2 W_2^T - W_1 W_1^T\|_{2 \rightarrow 2} &= \|W_2 W_2^T - W_1 W_2^T + W_1 W_2^T - W_1 W_1^T\|_{2 \rightarrow 2} \\ &\leq \|W_2\|_{2 \rightarrow 2} \|W_2 - W_1\|_{2 \rightarrow 2} + \|W_1\|_{2 \rightarrow 2} \|W_2 - W_1\|_{2 \rightarrow 2} \implies \end{aligned}$$

$$\|W_2 W_2^T - W_1 W_1^T\|_{2 \rightarrow 2} \leq 2\Lambda \|W_2 - W_1\|_{2 \rightarrow 2}. \quad (77)$$

Hence, we substitute the latter into (76), yielding

$$\begin{aligned} & \|G_{2,k-1}^1 - G_{1,k-1}^1\|_{2 \rightarrow 2} + \|G_{2,k-1}^2 - G_{1,k-1}^2\|_{2 \rightarrow 2} \\ & \leq 2\Lambda c_{1,k-1} \|W_2 - W_1\|_{2 \rightarrow 2} + \|A\|_{2 \rightarrow 2} \|W_2 - W_1\|_{2 \rightarrow 2} (c_{1,k-1} + c_{2,k-1}) \implies \end{aligned}$$

$$\begin{aligned} & \|G_{2,k-1}^1 - G_{1,k-1}^1\|_{2 \rightarrow 2} + \|G_{2,k-1}^2 - G_{1,k-1}^2\|_{2 \rightarrow 2} \\ & \leq (2\Lambda c_{1,k-1} + \|A\|_{2 \rightarrow 2} (c_{1,k-1} + c_{2,k-1})) \|W_2 - W_1\|_{2 \rightarrow 2}. \end{aligned} \quad (78)$$

Estimation of $\|B_{2,k-1}^1 - B_{1,k-1}^1\|_F$.

$$\begin{aligned} \|B_{2,k-1}^1 - B_{1,k-1}^1\|_F &\leq \theta_{k-1}^{-1} t_{k-1}^1 \|X_0\|_F \|W_2 - W_1\|_{2 \rightarrow 2} \\ &\leq \mu c_{1,k-1} \|A\|_{2 \rightarrow 2} \|Y\|_F \|W_2 - W_1\|_{2 \rightarrow 2}. \end{aligned} \quad (79)$$

Now, we substitute (74), (78), (79) into (73) and apply Lemma 4.2, to get

$$\begin{aligned} & \|f_{W_2}^k(Y) - f_{W_1}^k(Y)\|_F \leq \Gamma_{k-1} \|f_{W_2}^{k-1}(V) - f_{W_1}^{k-1}(V)\|_F \\ & + 2 \|f_{W_2}^{k-1}(V)\|_F [2\Lambda c_{1,k-1} + \|A\|_{2 \rightarrow 2} (c_{1,k-1} + c_{2,k-1})] \|W_2 - W_1\|_{2 \rightarrow 2} \\ & + 2\mu c_{1,k-1} \|X_0\|_F \|W_2 - W_1\|_{2 \rightarrow 2} \\ & \leq \Gamma_{k-1} \|f_{W_2}^{k-1}(V) - f_{W_1}^{k-1}(V)\|_F + [2\Delta_{k-1} (2\Lambda c_{1,k-1} + \|A\|_{2 \rightarrow 2} (c_{1,k-1} + c_{2,k-1})) \\ & + 2\mu c_{1,k-1} \|A\|_{2 \rightarrow 2} \|Y\|_F] \|W_2 - W_1\|_{2 \rightarrow 2}, \end{aligned}$$

where

$$\begin{aligned} \Delta_k &= 2\mu \|Y\|_F \left[\sum_{i=0}^{k-1} \left(\|A\|_{2 \rightarrow 2} (c_{1,i-1} \Lambda + c_{2,i-1} \|A\|_{2 \rightarrow 2}) + c_{2,i-1} \right) \right. \\ & \quad \left. \cdot \prod_{j=i}^{k-1} \Gamma_j \right] + \|A\|_{2 \rightarrow 2} (c_{1,k-1} \Lambda + c_{2,k-1} \|A\|_{2 \rightarrow 2}) + c_{2,k-1}, \end{aligned} \quad (80)$$

$$\Delta_0 = 0.$$

Now, we set

$$E_k = 2\Delta_{k-1}(2\Lambda c_{1,k-1} + \|A\|_{2 \rightarrow 2}(c_{1,k-1} + c_{2,k-1})) + 2\mu c_{1,k-1}\|A\|_{2 \rightarrow 2}\|Y\|_F,$$

thus

$$\begin{aligned} \|f_{W_2}^k(Y) - f_{W_1}^k(Y)\|_F &\leq \Gamma_{k-1}\|f_{W_2}^{k-1}(V) - f_{W_1}^{k-1}(V)\|_F \\ &\quad + E_k\|W_2 - W_1\|_{2 \rightarrow 2} \end{aligned} \quad (81)$$

Using the abbreviations defined by Γ_k , Δ_k , E_k , the general formula for K_L in (49) is

$$K_L = \sum_{k=1}^L \left(\max_{0 \leq i \leq L-1} \Gamma_i \right)^{L-k} E_k \quad \text{for } L \geq 1. \quad (82)$$

Based on (81), we prove via induction that (49) holds for any number of layers $L \geq 1$, with K_L given by (82). For $L = 1$, we can directly calculate K_1 :

$$\begin{aligned} \|f_{W_2}^1(Y) - f_{W_1}^1(Y)\|_F &\leq 2t_0^1\|A\|_{2 \rightarrow 2}\|Y\|_F\|W_2 - W_1\|_{2 \rightarrow 2} \\ &= 2\underbrace{\theta_0^{-1}t_0^1}_{=1}\|A\|_{2 \rightarrow 2}\|Y\|_F\|W_2 - W_1\|_{2 \rightarrow 2} = 2\mu c_{1,0}\|A\|_{2 \rightarrow 2}\|Y\|_F\|W_2 - W_1\|_{2 \rightarrow 2}, \end{aligned}$$

so that $2\mu c_{1,0}\|A\|_{2 \rightarrow 2}\|Y\|_F = E_1 = K_1$ as claimed in (82). Now, let us assume (49) holds for some $L \in \mathbb{N}$. Then, applying the estimate that appears in (81) for $L + 1$:

$$\begin{aligned} \|f_{W_2}^{L+1}(Y) - f_{W_1}^{L+1}(Y)\|_F &\leq \Gamma_L\|f_{W_2}^L(Y) - f_{W_1}^L(Y)\|_F + E_{L+1}\|W_2 - W_1\|_F \\ &\leq (\Gamma_L K_L + E_{L+1})\|W_2 - W_1\|_F \leq \left[\left(\max_{0 \leq i \leq L} \Gamma_i \right) K_L + E_{L+1} \right] \|W_2 - W_1\|_F \\ &= \left[\left(\max_{0 \leq i \leq L} \Gamma_i \right) \sum_{k=1}^L \left(\max_{0 \leq i \leq L-1} \Gamma_i \right)^{L-k} E_k + E_{L+1} \right] \|W_2 - W_1\|_F \\ &\leq \left(\sum_{k=1}^L \left(\max_{0 \leq i \leq L} \Gamma_i \right)^k E_k + \left(\max_{0 \leq i \leq L} \Gamma_i \right)^0 E_{L+1} \right) \|W_2 - W_1\|_F \\ &= \left(\sum_{k=1}^{L+1} \left(\max_{0 \leq i \leq L} \Gamma_i \right)^{L+1-k} E_k \right) \|W_2 - W_1\|_F = K_{L+1}\|W_2 - W_1\|_F. \end{aligned}$$

We successfully calculated the desired K_L . Now, under the additional assumptions $\{c_{1,k}\}_{k \geq 0}$, $\{c_{2,k}\}_{k \geq 0} \leq 1$, we may apply the ‘‘in particular’’ part of Lemma 4.2 on (50), to obtain a simplified upper bound on K_L . Thus, for γ and ζ_k defined in Lemmata 4.1 and 4.2 respectively, we have

$$\begin{aligned} K_L &\leq 2\mu\|Y\|_F \left[\mu^{-1}\|A\|_{2 \rightarrow 2} + \sum_{k=2}^L \left(\gamma^{L-k} \left(4\|A\|_{2 \rightarrow 2}((\Lambda + \|A\|_{2 \rightarrow 2}) + 1) \right. \right. \right. \\ &\quad \left. \left. \left. \cdot (\Lambda + \|A\|_{2 \rightarrow 2}) \right) (\zeta_{k-1} + 1) + \|A\|_{2 \rightarrow 2} \right) \right]. \end{aligned}$$

In the latter, we set $Z = 4\|A\|_{2 \rightarrow 2}((\Lambda + \|A\|_{2 \rightarrow 2}) + 1)(\Lambda + \|A\|_{2 \rightarrow 2})$ for the sake of brevity, so that

$$K_L \leq 2\mu\|Y\|_F \left[\|A\|_{2 \rightarrow 2}(\mu^{-1} + (L - 1)) + Z\gamma^L \sum_{k=2}^L \left(\gamma^{-k}(\zeta_{k-1} + 1) \right) \right].$$

Now, plugging (47) in the latter yields

$$\begin{aligned} K_L &\leq 2\mu\|Y\|_F \left[\|A\|_{2 \rightarrow 2}(\mu^{-1} + (L - 1)) + Z\gamma^L \sum_{k=2}^L \gamma^{-k} \left(\frac{\gamma^{k-1} - 1}{\gamma - 1} + 1 \right) \right] \\ &= 2\mu\|Y\|_F \left[\|A\|_{2 \rightarrow 2}(\mu^{-1} + (L - 1)) + \frac{Z\gamma^L}{\gamma - 1} \sum_{k=2}^L \left(\frac{1}{\gamma} - \frac{2}{\gamma^k} + \frac{\gamma}{\gamma^k} \right) \right] \\ &= 2\mu\|Y\|_F \left[\|A\|_{2 \rightarrow 2}(\mu^{-1} + (L - 1)) + \frac{Z\gamma^L}{\gamma - 1} \left(\frac{L-2}{\gamma} + (\gamma - 2) \sum_{k=2}^L \frac{1}{\gamma^k} \right) \right] \\ &= 2\mu\|Y\|_F \left[\|A\|_{2 \rightarrow 2}(\mu^{-1} + (L - 1)) + \frac{Z\gamma^L}{\gamma - 1} \left(\frac{L-2}{\gamma} + (\gamma - 2) \frac{\gamma^{1-L} - 1}{\gamma^{-1} - 1} \right) \right] \\ &= 2\mu\|Y\|_F \left[\|A\|_{2 \rightarrow 2}(\mu^{-1} + (L - 1)) \right. \\ &\quad \left. + \frac{Z}{\gamma - 1} \left(\frac{\gamma^L(L-2)}{\gamma} + \frac{\gamma(\gamma - 2)(\gamma^L - \gamma)}{\gamma - 1} \right) \right] \\ &< 2\mu\|Y\|_F \left[\|A\|_{2 \rightarrow 2}(\mu^{-1} + (L - 1)) \right. \\ &\quad \left. + Z \frac{\left(\gamma^L \left((L-2) + \gamma^2(\gamma - 2) \right) - \gamma^2(\gamma - 2) \right)}{\gamma - 1} \right]. \end{aligned} \tag{83}$$

The proof follows. \square

References

- [1] E. J. Candès, J. Romberg, and T. Tao. “Robust uncertainty principles: Exact signal reconstruction from highly incomplete frequency information”. In: *IEEE Transactions on information theory* 52.2 (2006), pp. 489–509.
- [2] I. Daubechies, M. Defrise, and C. De Mol. “An iterative thresholding algorithm for linear inverse problems with a sparsity constraint”. In: *Communications on Pure and Applied Mathematics: A Journal Issued by the Courant Institute of Mathematical Sciences* 57.11 (2004), pp. 1413–1457.

- [3] R. Chartrand and W. Yin. “Iteratively reweighted algorithms for compressive sensing”. In: *2008 IEEE international conference on acoustics, speech and signal processing*. IEEE. 2008, pp. 3869–3872.
- [4] S. Boyd, N. Parikh, and E. Chu. *Distributed optimization and statistical learning via the alternating direction method of multipliers*. Now Publishers Inc, 2011.
- [5] H. Yao et al. “Dr2-net: Deep residual reconstruction network for image compressive sensing”. In: *Neurocomputing* 359 (2019), pp. 483–493.
- [6] G. Yang et al. “DAGAN: Deep de-aliasing generative adversarial networks for fast compressed sensing MRI reconstruction”. In: *IEEE transactions on medical imaging* 37.6 (2017), pp. 1310–1321.
- [7] J. R. Hershey, J. Le Roux, and F. Weninger. “Deep unfolding: Model-based inspiration of novel deep architectures”. In: *arXiv preprint arXiv:1409.2574* (2014).
- [8] V. Monga, Y. Li, and Y. C Eldar. “Algorithm unrolling: Interpretable, efficient deep learning for signal and image processing”. In: *IEEE Signal Processing Magazine* 38.2 (2021), pp. 18–44.
- [9] K. Gregor and Y. LeCun. “Learning fast approximations of sparse coding”. In: *Proceedings of the 27th international conference on international conference on machine learning*. 2010, pp. 399–406.
- [10] J. Zhang et al. “Deep Unfolding With Weighted l_2 Minimization for Compressive Sensing”. In: *IEEE Internet of Things Journal* 8.4 (2020), pp. 3027–3041.
- [11] C. Bertocchi et al. “Deep unfolding of a proximal interior point method for image restoration”. In: *Inverse Problems* 36.3 (2020), p. 034005.
- [12] Y. Yang et al. “A Robust Deep Unfolded Network for Sparse Signal Recovery from Noisy Binary Measurements”. In: *2020 28th European Signal Processing Conference (EUSIPCO)*. IEEE. 2021, pp. 2060–2064.
- [13] A. P. Sabulal and S. Bhashyam. “Joint Sparse Recovery Using Deep Unfolding With Application to Massive Random Access”. In: *ICASSP 2020 - 2020 IEEE International Conference on Acoustics, Speech and Signal Processing (ICASSP)*. 2020, pp. 5050–5054. DOI: [10.1109/ICASSP40776.2020.9053312](https://doi.org/10.1109/ICASSP40776.2020.9053312).
- [14] M. Borgerding, P. Schniter, and S. Rangan. “AMP-Inspired Deep Networks for Sparse Linear Inverse Problems”. In: *IEEE Transactions on Signal Processing* 65.16 (2017), pp. 4293–4308. DOI: [10.1109/TSP.2017.2708040](https://doi.org/10.1109/TSP.2017.2708040).
- [15] J. Zhang and B. Ghanem. “ISTA-Net: Interpretable optimization-inspired deep network for image compressive sensing”. In: *Proceedings of the IEEE conference on computer vision and pattern recognition*. 2018, pp. 1828–1837.

- [16] Y. Khalifa, Z. Zhang, and E. Sejdić. “Sparse recovery of time-frequency representations via recurrent neural networks”. In: *2017 22nd International Conference on Digital Signal Processing (DSP)*. IEEE. 2017, pp. 1–5.
- [17] Y. Yang et al. “ADMM-Net: A deep learning approach for compressive sensing MRI”. In: *arXiv preprint arXiv:1705.06869* (2017).
- [18] P. Xiao, B. Liao, and N. Deligiannis. “Deepfpc: A deep unfolded network for sparse signal recovery from 1-bit measurements with application to doa estimation”. In: *Signal Processing* 176 (2020), p. 107699.
- [19] D. L. Donoho, A. Maleki, and A. Montanari. “Message-passing algorithms for compressed sensing”. In: *Proceedings of the National Academy of Sciences* 106.45 (2009), pp. 18914–18919.
- [20] E. T. Hale, W. Yin, and Y. Zhang. “Fixed-point continuation applied to compressed sensing: implementation and numerical experiments”. In: *Journal of Computational Mathematics* (2010), pp. 170–194.
- [21] A. Behboodi, H. Rauhut, and E. Schnoor. “Compressive Sensing and Neural Networks from a Statistical Learning Perspective”. In: *arXiv preprint arXiv:2010.15658* (2020).
- [22] Y. Shen et al. “Image reconstruction algorithm from compressed sensing measurements by dictionary learning”. In: *Neurocomputing* 151 (2015), pp. 1153–1162.
- [23] Z. Li, H. Huang, and S. Misra. “Compressed sensing via dictionary learning and approximate message passing for multimedia Internet of Things”. In: *IEEE Internet of Things Journal* 4.2 (2016), pp. 505–512.
- [24] H. Zayyani, M. Korki, and F. Marvasti. “Dictionary learning for blind one bit compressed sensing”. In: *IEEE Signal Processing Letters* 23.2 (2015), pp. 187–191.
- [25] R. Fu et al. “Theoretical Linear Convergence of Deep Unfolding Network for Block-Sparse Signal Recovery”. In: *arXiv preprint arXiv:2111.09801* (2021).
- [26] X. Chen et al. “Theoretical linear convergence of unfolded ISTA and its practical weights and thresholds”. In: *arXiv preprint arXiv:1808.10038* (2018).
- [27] E. Schnoor, A. Behboodi, and H. Rauhut. “Generalization Error Bounds for Iterative Recovery Algorithms Unfolded as Neural Networks”. In: *arXiv preprint arXiv:2112.04364* (2021).
- [28] B. Joukovsky et al. “Generalization error bounds for deep unfolding RNNs”. In: *Uncertainty in Artificial Intelligence*. PMLR. 2021, pp. 1515–1524.
- [29] C. Ma et al. “Rademacher complexity and the generalization error of residual networks”. In: *Communications in Mathematical Sciences* 18.6 (2020), pp. 1755–1774.

- [30] V. Vapnik. *The nature of statistical learning theory*. Springer science & business media, 1999.
- [31] S. Shalev-Shwartz et al. “Learnability, stability and uniform convergence”. In: *The Journal of Machine Learning Research* 11 (2010), pp. 2635–2670.
- [32] Huan Xu and Shie Mannor. “Robustness and generalization”. In: *Machine learning* 86.3 (2012), pp. 391–423.
- [33] V. Kouni et al. “ADMM-DAD Net: A Deep Unfolding Network for Analysis Compressed Sensing”. In: *ICASSP 2022 - 2022 IEEE International Conference on Acoustics, Speech and Signal Processing (ICASSP)*. 2022, pp. 1506–1510. DOI: [10.1109/ICASSP43922.2022.9747096](https://doi.org/10.1109/ICASSP43922.2022.9747096).
- [34] M. Kabanava and H. Rauhut. “Analysis l_1 -recovery with frames and gaussian measurements”. In: *Acta Applicandae Mathematicae* 140.1 (2015), pp. 173–195.
- [35] H. Cherkaoui et al. “Analysis vs synthesis-based regularization for combined compressed sensing and parallel MRI reconstruction at 7 tesla”. In: *2018 26th European Signal Processing Conference (EUSIPCO)*. IEEE. 2018, pp. 36–40.
- [36] Y. LeCun et al. “Gradient-based learning applied to document recognition”. In: *Proceedings of the IEEE* 86.11 (1998), pp. 2278–2324.
- [37] S. R. Becker, E. J. Candès, and M. C. Grant. “Templates for convex cone problems with applications to sparse signal recovery”. In: *Mathematical programming computation* 3.3 (2011), pp. 165–218.
- [38] S. Foucart and H. Rauhut. “An invitation to compressive sensing”. In: *A mathematical introduction to compressive sensing*. Springer, 2013, pp. 1–39.
- [39] M. Elad. “Sparse and redundant representations: from theory to applications in signal and image processing”. In: (2010).
- [40] S. Pejoski, V. Kafedziski, and D. Gleich. “Compressed sensing MRI using discrete nonseparable shearlet transform and FISTA”. In: *IEEE Signal Processing Letters* 22.10 (2015), pp. 1566–1570.
- [41] C. Li and B. Adcock. “Compressed sensing with local structure: uniform recovery guarantees for the sparsity in levels class”. In: *Applied and Computational Harmonic Analysis* 46.3 (2019), pp. 453–477.
- [42] P. T. Dao, A. Griffin, and X. J. Li. “Compressed sensing of EEG with Gabor dictionary: Effect of time and frequency resolution”. In: *2018 40th annual international conference of the IEEE engineering in medicine and biology society (EMBC)*. IEEE. 2018, pp. 3108–3111.
- [43] S.-J. Kim et al. “An Efficient Method for Compressed Sensing”. In: *2007 IEEE International Conference on Image Processing*. Vol. 3. 2007, pp. III – 117-III –120. DOI: [10.1109/ICIP.2007.4379260](https://doi.org/10.1109/ICIP.2007.4379260).

- [44] I. Daubechies, M. Defrise, and C. De Mol. “An iterative thresholding algorithm for linear inverse problems with a sparsity constraint”. In: *Communications on Pure and Applied Mathematics: A Journal Issued by the Courant Institute of Mathematical Sciences* 57.11 (2004), pp. 1413–1457.
- [45] M. Genzel, G. Kutyniok, and M. März. “ l_1 -Analysis minimization and generalized (co-) sparsity: When does recovery succeed?” In: *Applied and Computational Harmonic Analysis* 52 (2021), pp. 82–140.
- [46] E. J. Candes et al. “Compressed sensing with coherent and redundant dictionaries”. In: *Applied and Computational Harmonic Analysis* 31.1 (2011), pp. 59–73.
- [47] M. Kabanava and H. Rauhut. “Cosparsity in compressed sensing”. In: *Compressed Sensing and Its Applications*. Springer, 2015, pp. 315–339.
- [48] V. Kouni and H. Rauhut. “Spark Deficient Gabor Frame Provides A Novel Analysis Operator For Compressed Sensing”. In: *Neural Information Processing*. Ed. by T. Mantoro et al. Cham: Springer International Publishing, 2021, pp. 700–708. ISBN: 978-3-030-92310-5.
- [49] A. Maurer. “A vector-contraction inequality for rademacher complexities”. In: *International Conference on Algorithmic Learning Theory*. Springer, 2016, pp. 3–17.
- [50] R. Vershynin. *High-dimensional probability: An introduction with applications in data science*. Vol. 47. Cambridge university press, 2018.
- [51] A. Krizhevsky et al. “Learning multiple layers of features from tiny images”. In: (2009).
- [52] N. Ketkar. “Introduction to pytorch”. In: *Deep learning with python*. Springer, 2017, pp. 195–208.
- [53] D. P. Kingma and J. Ba. “Adam: A method for stochastic optimization”. In: *arXiv preprint arXiv:1412.6980* (2014).
- [54] L. Prechelt. “Early stopping-but when?” In: *Neural Networks: Tricks of the trade*. Springer, 1998, pp. 55–69.
- [55] P. Kittipoom, G. Kutyniok, and W. Q. Lim. “Construction of compactly supported shearlet frames”. In: *Constructive Approximation* 35.1 (2012), pp. 21–72.